Chapter 2
Definition of Different Types of Finite Elements

Abstract This chapter presents a wide variety of finite elements of different shapes (quadrilaterals, hexahedra, triangles, tetrahedra, pyramids and wedges) useful for the numerical resolution of wave equations. More precisely, the H1, H(curl) and H(div) conforming finite elements are described in details by focusing on their spectral version which induces the important concept of mass-lumping for quadrilaterals and hexahedra. This concept enables us to construct performant algorithms.

2.1 1D Mass-Lumping and Spectral Elements

2.1.1 A Complex Solution for a Simple Problem

We can get the exact solution of the 1D wave equation:
Find $u : \mathbb{R}\times]0, T[\to \mathbb{R}$ such that:

$$\frac{\partial^2 u}{\partial t^2}(x,t) - c^2 \frac{\partial^2 u}{\partial x^2}(x,t) = 0 \quad \text{in } \mathbb{R}\times]0,T[, \tag{2.1a}$$

$$u(x,0) = u_0(x), \qquad \frac{\partial u}{\partial t}(x,0) = u_1(x) \quad \text{in } \mathbb{R}, \tag{2.1b}$$

by using a centered second-order finite difference method with a CFL equal to 1 (i.e. $c\Delta t/h = 1$, where Δt and h are the time-step and the space-step respectively).

Although simple, this solution does not hold in higher dimensions and finite difference methods are not satisfactory for complex domains. This is the reason why we are going to construct a finite element method to solve (2.1a) and (2.1b). For this purpose, we first write the variational formulation of this equation:
Find $u(.,t) \in H^1(\mathbb{R}), t \in]0,T[$ such that:

$$\frac{\mathrm{d}^2}{\mathrm{d}t^2}\int_{\mathbb{R}} u\, v\, \mathrm{d}x \;+\; c^2 \int_{\mathbb{R}} \frac{\partial u}{\partial x}\frac{\partial v}{\partial x}\mathrm{d}x = 0 \quad \forall v \in H^1(\mathbb{R}), \tag{2.2a}$$

G. Cohen and S. Pernet, *Finite Element and Discontinuous Galerkin Methods for Transient Wave Equations*, Scientific Computation,
DOI 10.1007/978-94-017-7761-2_2

$$u(x,0) = u_0(x), \qquad \frac{\partial u}{\partial t}(x,0) = u_1(x) \quad \text{in } \mathbb{R}. \tag{2.2b}$$

For the moment, we only develop the semi-discretization in space of this problem. Approximation in time will be introduced later.

Let

$$V_h^r(\mathbb{R}) = \{v \in C^0(\mathbb{R}) \mid \forall p \in \mathbb{Z},\ v_{|[x_p, x_{p+1}]} \in P_r\} \cap H^1(\mathbb{R}), \tag{2.3}$$

where P_r is the space of polynomials of degree r or less on $\mathbb{R}$, be the (continuous) finite element space of rth-order associated with a mesh $\{[x_p, x_{p+1}]\}_{p\in\mathbb{Z}}$ of $\mathbb{R}$. We have $V_h^r(\mathbb{R}) \subset H^1(\mathbb{R})$ [1]. By using these notations, the semi-discretized formulation in space of (2.2a) and (2.2b) reads

Find $u_h(.,t) \in V_h^r(\mathbb{R})$, $t \in]0, T[$ such that:

$$\frac{\mathrm{d}^2}{\mathrm{d}t^2} \int_{\mathbb{R}} u_h v_h \mathrm{d}x + c^2 \int_{\mathbb{R}} \frac{\partial u_h}{\partial x} \frac{\partial v_h}{\partial x} \mathrm{d}x = 0, \quad \forall v_h \in V_h^r(\mathbb{R}), \tag{2.4a}$$

$$u_h(x,0) = u_0(x), \qquad \frac{\partial u_h}{\partial t}(x,0) = u_1(x) \quad \text{in } \mathbb{R}. \tag{2.4b}$$

For each segment $[x_p, x_{p+1}]$ of $\mathbb{R}$, we have a set of $r+1$ interpolation points which are its two ends $x_p = x_{p,1}$ and $x_{p+1} = x_{p,r+1}$ and $r-1$ (a priori) regularly spaced interior points denoted $x_{p,j}$, such that $x_{p,j+1} = x_p + j(x_{p+1} - x_p)/r$, $j = 1 \ldots r-1$. The degrees of freedom of the finite element method are the values of the functions of $V_h^r(\mathbb{R})$ at these interpolation points. The restriction to an interval $[x_p, x_{p+1}]$ of a basis function of $V_h^r(\mathbb{R})$ corresponding to a degree of freedom located at the point $x_{p,j}$ is defined by the Lagrange polynomial $\varphi_{p,j}(x)$ defined as

$$\varphi_{p,j}(x) = \frac{\displaystyle\prod_{\ell=1,\ell\neq j}^{r+1} (x - x_{p,\ell})}{\displaystyle\prod_{\ell=1,\ell\neq j}^{r+1} (x_{p,j} - x_{p,\ell})}, \quad j = 1 \ldots r+1. \tag{2.5}$$

By taking basis functions λ_i based on (2.5) for v_h and computing all the integrals of (2.4a), we get the discrete system

$$M_{1,r} \frac{\mathrm{d}^2 \underline{U}}{\mathrm{d}t^2}(t) + K_{1,r}\, \underline{U}(t) = 0, \tag{2.6}$$

with

$$(M_{1,r})_{\ell,m} = \int_{\mathbb{R}} \lambda_\ell(x)\, \lambda_m(x)\, \mathrm{d}x, \tag{2.7a}$$

$$(K_{1,r})_{\ell,m} = \int_{\mathbb{R}} \frac{\partial \lambda_\ell}{\partial x} \frac{\partial \lambda_m}{\partial x} \mathrm{d}x, \ (\ell, m) \in \mathbb{Z}^2, \tag{2.7b}$$

$$\underline{U}^T = (u_q, u_{q,1}, \ldots, u_{q,r-1})_{q\in\mathbb{Z}}. \tag{2.7c}$$

$M_{1,r}$ is the *mass matrix* and $K_{1,r}$ is the *stiffness matrix* of the discrete problem. By using a centered second-order scheme in time, we get

$$M_{1,r}\,\frac{\underline{U}^{n+1} - 2\underline{U}^n + \underline{U}^{n-1}}{\Delta t^2} \;+\; K_{1,r}\,\underline{U}^n \;= 0. \tag{2.8}$$

From (2.8), we deduce

$$\underline{U}^{n+1} = 2\underline{U}^n - \underline{U}^{n-1} - \Delta t^2 M_{1,r}^{-1}\,K_{1,r}\,\underline{U}^n. \tag{2.9}$$

Now, $M_{1,r}$ is a symmetric $(2r+1)$-diagonal matrix that must be inverted at each time-step. Moreover, the number of diagonal rows grows for higher dimensions in space, which leads to a very costly algorithm.[1]

2.1.2 Mass-Lumping

A palliative to this inversion is to replace $M_{1,r}$ by a diagonal matrix. This can be done by using a technique of mass-lumping which consists of two steps:

1. Locate the interpolation points to the quadrature points,
2. Compute the mass integrals by using the corresponding quadrature rule.

Let us denote $\left(\xi_m^p\right)_{m=1}^{r+1}$ a set of quadrature points on $[x_p, x_{p+1}]$ and $\left(\omega_m^p\right)_{m=1}^{r+1}$ the corresponding weights. We have

$$\begin{aligned}\int_{x_p}^{x_{p+1}} u_h\varphi_{p,j}\mathrm{d}x &\simeq \sum_{\ell=1}^{r+1} u_{p,\ell}\int_{x_p}^{x_{p+1}} \varphi_{p,\ell}(x)\varphi_{p,j}(x)\mathrm{d}x\\ &\simeq \sum_{\ell=1}^{r+1} u_{p,\ell}\sum_{m=1}^{r+1}\omega_m^p\varphi_{p,\ell}(\xi_m^p)\varphi_{p,j}(\xi_m^p),\end{aligned} \tag{2.10}$$

where $u_{p,\ell}$ are the values of u_h at the quadrature points.

By taking $x_{p,m} = \xi_m^p$, we have $\varphi_{p,j}(\xi_m^p) = \delta_{j,m}$. So,

$$\int_{x_p}^{x_{p+1}} u_h\varphi_{p,j}\mathrm{d}x \simeq \sum_{\ell=1}^{r+1} u_{p,\ell}\sum_{m=1}^{r+1}\omega_m^p\delta_{\ell,m}\delta_{j,m} = \omega_j^p u_{p,j}, \tag{2.11}$$

which shows that conditions 1 and 2 ensure mass-lumping.

[1] The inverse of a n-diagonal matrix is not n-diagonal in general, which avoids the storage of $M_{1,r}^{-1}$. The correct approach would be to invert $M_{1,r}$ at each time-step by an iterative method. Since Δt is generally small, moving from t_n to t_{n+1} requires few iterations. However, each iteration is expensive compared to the product by a diagonal matrix.

An important point is to be sure that the error committed by using a quadrature rule is not greater than the error committed by the finite element method to keep the order of the approximation. The answer to this difficult question is given by Ciarlet in [1, 2] as follows: In order to keep the approximation of a finite element method of order r, one must use a quadrature rule at least exact for polynomials of P_{2r-1}.

A first candidate would be a Newton–Cotes quadrature rule, but such a rule is only exact for P_r with $r+1$ quadrature points. Moreover, for $r > 6$, some of their weights are negative, which induces some stability problems, as we shall see later.

Gauss quadrature rules are exact for P_{2r+1} with $r+1$ quadrature points, but they cannot include the ends of the intervals. However, they will be useful for discontinuous Galerkin methods, as shown in Chap. 4.

Actually, the good candidates are the Gauss-Lobatto rules which are exact for P_{2r-1} with $r+1$ quadrature points, which are the $r-1$ roots of the derivatives of the Legendre polynomial of order r (while Gauss points are the roots of the polynomials themselves) and the ends of the interval $[x_p, x_{p+1}]$. This technique of mass-lumping was first introduced independently in [3] for reservoir simulation and in [4] for neutronics and then renamed "spectral elements" [5]. It was then applied to the wave equation in [6, 7].

In Table 2.1, we give the exact values for $1 \leq r \leq 6$ and in Table 2.2, the approximate values for $7 \leq r \leq 10$ of the abscissae of the points and the corresponding weights of the Gauss-Lobatto rules when $x_p = 0$ and $x_{p+1} = 1$ on the semi-interval $[0, 1/2]$. The values on the interval $[1/2, 1]$ are deduced by symmetry.

In the same way, we give in Table 2.3 the exact values for $1 \leq r \leq 5$ and in Table 2.4, the approximate values for $6 \leq r \leq 9$ of the abscissae of the points and the corresponding weights of the Gauss rules when $x_p = 0$ and $x_{p+1} = 1$ on the semi-interval $[0, 1/2]$. Here also, the values on the interval $[1/2, 1]$ are deduced by symmetry.

The Gauss or Gauss-Lobatto points on an interval $[x_p, x_{p+1}]$ are deduced from those on the unit interval $[0, 1]$ by the following affine mapping:

$$F_p(\hat{x}) = (x_{p+1} - x_p)\hat{x} + x_p \tag{2.12}$$

and the weights are multiplied by $(x_{p+1} - x_p)$.

More details about mass-lumping can be found in [8].

Remark: We recall the definition of Legendre polynomials on the interval $[-1, 1]$

$$\begin{cases} L_0(x) = 1, \\ L_1(x) = x, \\ L_r(x) = \dfrac{(2r-1)}{r} x L_{r-1}(x) - \dfrac{(r-1)}{r} L_{r-2}(x), \quad \forall r > 1. \end{cases} \tag{2.13}$$

Table 2.1 Exact values of the abscissae of the points and of the weights of the Gauss-Lobatto quadrature rules for the semi-interval [0, 1/2] for $1 \leq r \leq 6$

	$j=1$	$j=2$	$j=3$	$j=4$
$r=1\,(\hat{\xi})$	0			
$r=1\,(\hat{\omega})$	$\frac{1}{2}$			
$r=2\,(\hat{\xi})$	0	$\frac{1}{2}$		
$r=2\,(\hat{\omega})$	$\frac{1}{6}$	$\frac{2}{3}$		
$r=3\,(\hat{\xi})$	0	$\frac{5-\sqrt{5}}{10}$		
$r=3\,(\hat{\omega})$	$\frac{1}{12}$	$\frac{5}{12}$		
$r=4\,(\hat{\xi})$	0	$\frac{7-\sqrt{21}}{14}$	$\frac{1}{2}$	
$r=4\,(\hat{\omega})$	$\frac{1}{20}$	$\frac{49}{180}$	$\frac{16}{45}$	
$r=5\,(\hat{\xi})$	0	$\frac{21-\sqrt{147+42\sqrt{7}}}{42}$	$\frac{21-\sqrt{147-42\sqrt{7}}}{42}$	
$r=5\,(\hat{\omega})$	$\frac{1}{30}$	$\frac{14-\sqrt{7}}{60}$	$\frac{14+\sqrt{7}}{60}$	
$r=6\,(\hat{\xi})$	0	$\frac{33-\sqrt{495+66\sqrt{15}}}{66}$	$\frac{33-\sqrt{495-66\sqrt{15}}}{66}$	$\frac{1}{2}$
$r=6\,(\hat{\omega})$	$\frac{1}{42}$	$\frac{31}{175}-\frac{\sqrt{15}}{100}$	$\frac{31}{175}+\frac{\sqrt{15}}{100}$	$\frac{128}{525}$

Table 2.2 Approximate values of the abscissae of the points and of the weights of the Gauss-Lobatto quadrature rules for the semi-interval [0, 1/2] for $7 \leq r \leq 10$

r	$\hat{\xi}$	$\hat{\omega}$	r	$\hat{\xi}$	$\hat{\omega}$
7	0	0.017 857 143	9	0	0.011 111 111
	0.064 129 926	0.105 352 114		0.040 233 046	0.066 652 995
	0.204 149 909	0.170 561 346		0.130 613 067	0.112 444 671
	0.395 350 391	0.206 229 397		0.261 037 525	0.146 021 342
				0.417 360 521	0.163 769 881
8	0	0.013 888 889	10	0	0.009 090 909
	0.055 012 100	0.082 747 681		0.032 999 285	0.054 806 137
	0.161 406 860	0.137 269 356		0.107 758 263	0.093 584 941
	0.318 441 268	0.173 214 255		0.217 382 337	0.124 024 052
	0.5	0.185 759 637		0.352 120 932	0.143 439 562
				0.5	0.150 108 798

Table 2.3 Exact values of the abscissae of the points and of the weights of the Gauss quadrature rules for the semi-interval [0, 1/2]

	$j=1$	$j=2$	$j=3$
$r=1\,(\hat{\xi})$	$\frac{1}{2}$		
$r=1\,(\hat{\omega})$	1		
$r=2\,(\hat{\xi})$	$\frac{3-\sqrt{3}}{6}$		
$r=2\,(\hat{\omega})$	$\frac{1}{2}$		
$r=3\,(\hat{\xi})$	$\frac{5-\sqrt{15}}{10}$	$\frac{1}{2}$	
$r=3\,(\hat{\omega})$	$\frac{5}{18}$	$\frac{4}{9}$	
$r=4\,(\hat{\xi})$	$\frac{35-\sqrt{525+70\sqrt{30}}}{70}$	$\frac{35-\sqrt{525-70\sqrt{30}}}{70}$	
$r=4\,(\hat{\omega})$	$\frac{18-\sqrt{30}}{72}$	$\frac{18+\sqrt{30}}{72}$	
$r=5\,(\hat{\xi})$	$\frac{21-\sqrt{245+14\sqrt{70}}}{42}$	$\frac{21-\sqrt{245-14\sqrt{70}}}{42}$	$\frac{1}{2}$
$r=5\,(\hat{\omega})$	$\frac{322-13\sqrt{70}}{1800}$	$\frac{322+13\sqrt{70}}{1800}$	$\frac{64}{225}$

Table 2.4 Approximate values of the abscissae of the points and of the weights of the Gauss quadrature rules for the semi-interval [0, 1/2] for $6 \le r \le 9$

r	$\hat{\xi}$	$\hat{\omega}$	r	$\hat{\xi}$	$\hat{\omega}$
6	0.033 765 243	0.085 662 246	8	0.019 855 072	0.050 614 268
	0.169 395 307	0.180 380 787		0.101 666 761	0.111 190 517
	0.380 690 407	0.233 956 967		0.237 233 795	0.156 853 323
				0.408 282 679	0.181 341 892
7	0.025 446 044	0.064 742 483	9	0.015 919 880	0.040 637 194
	0.129 234 407	0.139 852 696		0.081 984 446	0.090 324 080
	0.297 077 424	0.190 915 025		0.193 314 284	0.130 305 348
	0.5	0.208 979 592		0.337 873 288	0.156 173 539
				0.5	0.165 119 677

2.1.3 Spectral Elements

The above defined mass-lumping technique can be seen from a different point of view: In fact, the Gauss or Gauss-Lobatto points avoid the Runge phenomenon. This phenomenon is classically illustrated in the following way:

If you want to interpolate the function $f = 1/(x^2 + 1)$ on an interval containing $[-5, 5]$ by using Lagrange polynomials defined on regularly spaced points, the norm of the resulting polynomial grows with the order of interpolation. Actually, the Lagrange polynomial coincides with f at all the interpolation points but oscillates more and more between these points at the ends of the interval, as shown in Fig. 2.1.

From a theoretical point of view, avoiding Runge phenomenon depends on the minimization of the supremum norm $||.||_\infty$ of the difference of a function f and its rth-order interpolation denoted $\mathscr{I}_r^1 f$ over an interval $I_1 = [a, b]$. In practice, this minimum p^* is not obtained, but one can get an approximative knowledge by using the inequality

$$||f(x) - \mathscr{I}_r^1 f(x)||_\infty \leq [1 + \Lambda(\Pi_r^1)]\, ||f(x) - p^*(x)||_\infty, \tag{2.14}$$

where Π_r^1 is a given set of $r + 1$ points and

$$\Lambda(\Pi_r^1) = \max_{x \in I_1} \sum_{i=1}^{r+1} |L_i(\Pi_r^1, x)|, \tag{2.15}$$

L_i being a Lagrange polynomial on interval I_1.

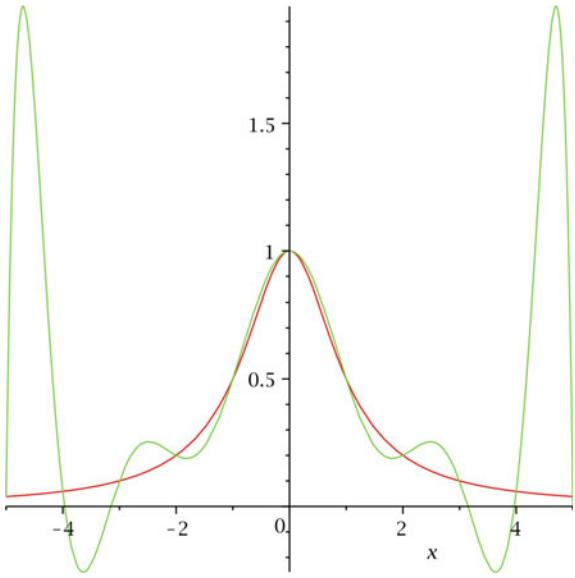

Fig. 2.1 Tenth order Lagrange polynomial interpolation on regularly spaced points of $f = 1/(x^2 + 1)$ on $[-5, 5]$ (in *green*) compared to the function (in *red*)

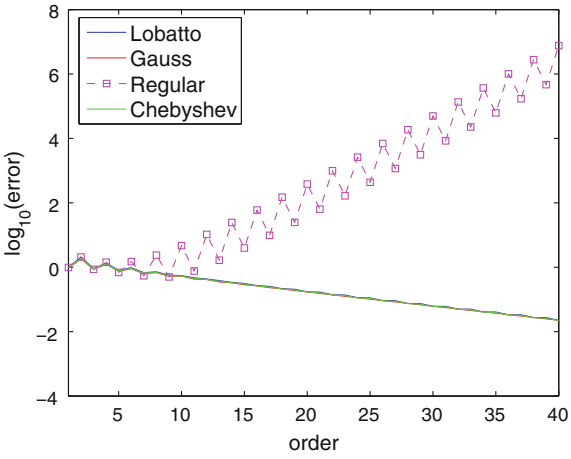

Fig. 2.2 L^2-norm logarithmic error of a Lagrange interpolation of f by polynomials of order 1 to 40 using different kinds of points. One can notice the exponential divergence of the regularly-spaced points

$\Lambda(\Pi_r^1)$ is called the Lebesgue constant. The approximation $\mathscr{I}_r^1 f$ is all the better that this constant is small. More details and references on this process can be found in [9, 10].

A classical answer to this problem was to use Chebyshev points to avoid these oscillations. For a long time, these points were regarded as the "optimal" ones and, since they enabled an exponential convergence in r of the methods, a Lagrange interpolation using Chebyshev points was defined as a "spectral element method" [11]. Unfortunately, Chebyshev points cannot support an efficient quadrature formula.

The question can be asked: is the use of Gauss or Gauss-Lobatto points for Lagrange interpolation able to get the so-called spectral convergence? A first answer is given by the good behaviour of their Lebesgue coefficients [9]. On the other hand, we interpolated f by using Chebyshev, Gauss and Gauss-Lobatto points on interval $[-5, 5]$ and we had very similar results for the three kinds of points as shown in Fig. 2.2.

In all the following, spectral elements will implicitly denote finite elements whose interpolation points coincide with quadrature points for quadrilaterals or hexahedra and elements with "optimal" nodes for other elements.

2.1.4 Nodal and Modal Elements

The construction of basis functions in this section corresponds to a "nodal" approach, i.e. the basis functions are defined by their values at the nodes of the elements. In this approach, the degrees of freedom are the values of the functions at these nodes. This enables us to get continuous finite element methods by enforcing the solution to have a unique value at the boundaries nodes (when they exist). However, as we shall see later, this type of elements can also be used for discontinuous formulations.

Another approach is to use basis functions corresponding to other criteria (for instance, values of linear forms [2] or orthogonal basis [12]). Then, the solution is given by a linear combination of the basis functions whose coefficients do not represent values of the functions. This approach, called the "modal" approach, leads to discontinuous formulations in general but can provide partially continuous elements in some cases, as in mixed formulations which will be introduced below.

The following three sections deal with nodal elements.

2.2 Quadrilaterals and Hexahedra

As we said in the previous section, our purpose is to solve wave equations on complex geometries in an efficient way. For this reason, we want to extend the concept of our spectral element approach to higher dimensions. This must be done in two steps:

1. Define a spectral unit element.
2. Extend this definition to any element.

As we shall see, the appropriate unit elements in 2D and 3D are the unit square $[0, 1]^2$ and unit cube $[0, 1]^3$ respectively. Before defining the approximation, let us first define the Gauss or Gauss-Lobatto quadrature rules for these unit elements, which is denoted $\widehat{K}$ in the following.

2.2.1 Higher-Dimensional Tensor Quadrature Rules

Let us first study the 2D case. We want to integrate an integrable function $f : \mathbb{R}^2 \to \mathbb{R}$ on the unit square by using a 1D quadrature rule on $[0, 1]$ whose quadrature points are $\left(\hat{\xi}_p\right)_{p=1}^{r+1}$ and whose weights are $\left(\hat{\omega}_p\right)_{p=1}^{r+1}$. By using Fubini's theorem, we have

$$\begin{aligned}
\int_{\widehat{K}} f(\underline{\hat{x}})\,\mathrm{d}\underline{\hat{x}} &= \int_0^1 \int_0^1 f(\underline{\hat{x}})\,\mathrm{d}\underline{\hat{x}} = \int_0^1 \left(\int_0^1 f(\hat{x}_1, \hat{x}_2)\,\mathrm{d}\hat{x}_2 \right) \mathrm{d}\hat{x}_1 \\
&\simeq \int_0^1 \left(\sum_{q=1}^{r+1} \hat{\omega}_q f(\hat{x}_1, \hat{\xi}_q) \right) \mathrm{d}\hat{x}_1 \\
&\simeq \sum_{p=1}^{r+1} \hat{\omega}_p \left(\sum_{q=1}^{r+1} \hat{\omega}_q f(\hat{\xi}_p, \hat{\xi}_q) \right) \\
&= \sum_{p=1}^{r+1} \sum_{q=1}^{r+1} \hat{\omega}_p \hat{\omega}_q f(\hat{\xi}_p, \hat{\xi}_q) = \sum_{p=1}^{r+1} \sum_{q=1}^{r+1} \hat{\omega}_{p,q} f(\hat{\underline{\xi}}_{p,q}).
\end{aligned} \tag{2.16}$$

So, we see that we can define a 2D quadrature rule whose quadrature points are

$$- \left(\hat{\underline{\xi}}_{p,q} = (\hat{\xi}_p, \hat{\xi}_q)\right)_{(p,q)=(1,1)}^{(r+1,r+1)}$$

and whose weights are

$$- \left(\hat{\omega}_{p,q} = \hat{\omega}_p \hat{\omega}_q\right)_{(p,q)=(1,1)}^{(r+1,r+1)}.$$

Now, it is easy to see that, if this 1D quadrature rule is exact for polynomials of P_r, $r \in \mathbb{N}$, the corresponding 2D quadrature rule is exact for Q_r, where Q_r is the set of polynomials of degree r or less in each variable which reads, in dimension d:

$$Q_r = \left\{ v(\hat{\underline{x}}) = \sum_{\underline{j}=(j_1,\dots j_d)\in\{0,\dots r\}^d} a_{\underline{j}} \prod_{k=1}^{d} \hat{x}_k^{j_k},\ a_{\underline{j}} \in \mathbb{R} \right\}. \tag{2.17}$$

In fact, we can write for any monomial $\hat{x}_1^i \hat{x}_2^j$, so that $0 \le i \le r$ and $0 \le j \le r$,

$$\begin{aligned} \int_{\widehat{K}} \hat{x}_1^i \hat{x}_2^j \, \mathrm{d}\hat{\underline{x}} &= \int_0^1 \hat{x}_1^i \, \mathrm{d}\hat{x}_1 \times \int_0^1 \hat{x}_2^j \, \mathrm{d}\hat{x}_2 \\ &= \sum_{p=1}^{r+1} \hat{\omega}_p \hat{\xi}_p^i \sum_{q=1}^{r+1} \hat{\omega}_q \hat{\xi}_q^j = \sum_{p=1}^{r+1} \sum_{q=1}^{r+1} \hat{\omega}_{p,q} \hat{\xi}_p^i \hat{\xi}_q^j. \end{aligned} \tag{2.18}$$

In the same way, it is easy to show that the 3D quadrature rule whose quadrature points are

$$- \left(\hat{\underline{\xi}}_{p,q,s} = (\hat{\xi}_p, \hat{\xi}_q, \hat{\xi}_s)\right)_{(p,q,s)=(1,1,1)}^{(r+1,r+1,r+1)}$$

and whose weights are

$$- \left(\hat{\omega}_{p,q,s} = \hat{\omega}_p \hat{\omega}_q \hat{\omega}_s\right)_{(p,q,s)=(1,1,1)}^{(r+1,r+1;r+1)},$$

is a 3D extension of our 1D quadrature rule, exact for polynomials of Q_r.

2.2.2 *Tensor Unit Spectral Elements*

Basis functions on the unit element are classically defined as the product of 1D basis functions. So, if we denote by $\hat{\varphi}_i(\hat{x})$ the Lagrange polynomial defined in (2.5) in

which we set $x_p = 0$, $x_{p+1} = 1$ and $\hat{x} \in [0, 1]$ such that $\hat{\varphi}_i(\hat{\xi}_j) = \delta_{ij}$, we can define the basis functions $\hat{\varphi}_{\ell,m}(\hat{x}_1, \hat{x}_2)$ on the unit square as

$$\hat{\varphi}_{\ell,m}(\hat{x}_1, \hat{x}_2) = \hat{\varphi}_\ell(\hat{x}_1)\hat{\varphi}_m(\hat{x}_2), \tag{2.19}$$

and, in the same way, on the unit cube

$$\hat{\varphi}_{\ell,m,n}(\hat{x}_1, \hat{x}_2, \hat{x}_3) = \hat{\varphi}_\ell(\hat{x}_1)\hat{\varphi}_m(\hat{x}_2)\hat{\varphi}_n(\hat{x}_3), \tag{2.20}$$

where $1 \leq \ell,\ m,\ n \leq r + 1$.

Since $\hat{\varphi}_i \in P_r$, we have $\hat{\varphi}_{\ell,m} \in Q_r$ and $\hat{\varphi}_{\ell,m,n} \in Q_r$, with Q_r defined as in (2.17).

Obviously, we have

$$\hat{\varphi}_{\ell,m}(\hat{\underline{\xi}}_{i,j}) = \delta_{\ell,i}\,\delta_{m,j}, \tag{2.21a}$$

$$\hat{\varphi}_{\ell,m,n}(\hat{\underline{\xi}}_{i,j,k}) = \delta_{\ell,i}\,\delta_{m,j}\,\delta_{n,k}. \tag{2.21b}$$

Now, following Ciarlet's criteria given in [2], for a square or a cube, one must use a quadrature rule at least exact for polynomials of Q_{2r-1} in order to keep the approximation of finite element method of order r. So, using the results of the previous section, we see that the Gauss-Lobatto rule is still the good candidate for the unit elements in 2D and 3D. An example of Gauss-Lobatto points in 2D is given in Fig. 2.3.

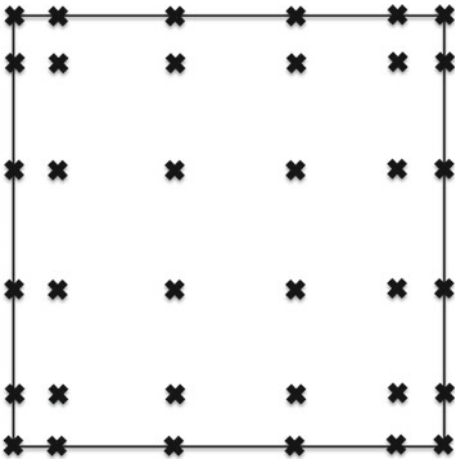

Fig. 2.3 Fifth-order Gauss-Lobatto points on the unit square

Remark: Even for non regularly-spaced, basis functions on the unit elements remain products of equations of lines or planes (parallel to the axes). This is not true for non tensor elements.

2.2.3 Extension to Quadrilaterals and Hexahedra

We extend our basis functions to a quadrilateral or an hexahedron K_i in a classical way (see for instance [2]) by using a mapping $\underline{F}_i = (F_i^{(1)}, \dots F_i^{(d)})^T$ such that

$$\underline{F}_i(\widehat{K}) = K_i. \tag{2.22}$$

The components $F_i^{(j)}$ of $\underline{F}_i$ are generally taken in Q_1, which provides quadrilaterals and hexahedra with straight edges.[2] However, one can also take these components in $Q_r, r > 1$. Such a choice leads to elements with curved edges (quadratic for $r = 2$, cubic for $r = 3$, etc.) which can be more accurate to approximate curved boundaries. In practice, we have, for $r = 1$ in 2D:

$$\underline{F}_i(\widehat{K})(\hat{x}_1, \hat{x}_2) = \sum_{\ell=1}^{2} \sum_{m=1}^{2} \underline{c}_{\ell,m}^{(i)} \hat{\varphi}_{\ell,m,}(\hat{x}_1, \hat{x}_2), \tag{2.23}$$

and, in 3D,

$$\underline{F}_i(\widehat{K})(\hat{x}_1, \hat{x}_2, \hat{x}_3) = \sum_{\ell=1}^{2} \sum_{m=1}^{2} \sum_{n=1}^{2} \underline{c}_{\ell,m,n}^{(i)} \hat{\varphi}_{\ell,m,n}(\hat{x}_1, \hat{x}_2, \hat{x}_3), \tag{2.24}$$

where $\underline{c}_{\ell,m}^{(i)}$ and $\underline{c}_{\ell,m,n}^{(i)}$ are the summits of K_i in 2D and 3D (Fig. 2.4).

As we said, $\underline{F}_i$ can be defined in the same way for $r > 1$ by using basis functions on $\widehat{K}$, provided the knowledge of the analytical definition of the edges of K_i and the use of the Gordon-Hall transform [13, 14].

One can easily see that, for $r = 1$, $\underline{F}_i$ is bilinear in 2D and trilinear in 3D[3] unlike mappings used for triangles and tetrahedra which are linear. This can be somehow troublesome since its Jacobian matrix and its Jacobian are not constant. This is a fortiori true for $r > 1$.

A basis functions φ on an element K_i is classically (for functions in H^1) defined as follows

$$\varphi = \hat{\varphi} \circ \underline{F}_i^{-1}, \tag{2.25}$$

where $\hat{\varphi}$ is a basis function on the unit element.

[2] But, of course, not plane faces for hexahedra, unless the summits of a face are coplanar.

[3] Unless all the faces are planes, which provides a linear mapping.

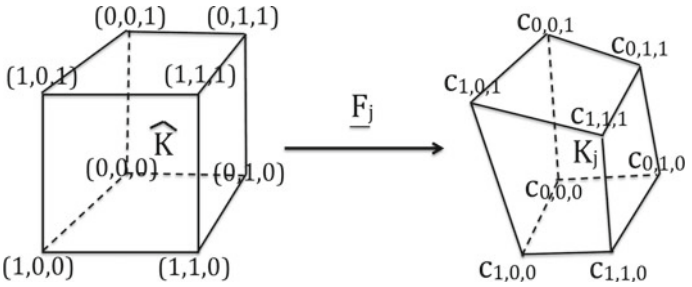

Fig. 2.4 The 3D mapping for $r = 1$

One can notice that such a definition provides basis functions which are in general no longer polynomial, since the components of $\underline{F}_i^{-1}$ are fractions involving polynomials and square roots of polynomials when $\underline{F}_i$ is not linear.

Now, the question can be asked: Does this definition of finite elements still provide mass-lumping?

To answer this question, we integrate the product of two basis functions $\varphi_{j,k}$ and $\varphi_{\ell,m}$ on K_i such that $\varphi_{j,k} = \hat{\varphi}_{j,k} \circ \underline{F}_i^{-1}$ and $\varphi_{\ell,m} = \hat{\varphi}_{\ell,m} \circ \underline{F}_i^{-1}$. By using (2.21a), we have

$$\begin{aligned}\int_{K_i} \varphi_{j,k}(\underline{x})\, \varphi_{\ell,m}(\underline{x}) \mathrm{d}\underline{x} &= \int_{\widehat{K}} |J_i(\underline{\hat{x}})|\, \hat{\varphi}_{j,k}(\underline{\hat{x}})\, \hat{\varphi}_{\ell,m}(\underline{\hat{x}})\, \mathrm{d}\underline{\hat{x}} \\ &\simeq \sum_{p=1}^{r+1} \sum_{q=1}^{r+1} \hat{\omega}_{p,q}\, |J_i(\underline{\hat{\xi}}_{p,q})|\, \hat{\varphi}_{j,k}(\underline{\hat{\xi}}_{p,q})\, \hat{\varphi}_{\ell,m}(\underline{\hat{\xi}}_{p,q}) \\ &= \sum_{p=1}^{r+1} \sum_{q=1}^{r+1} \hat{\omega}_{p,q}\, |J_i(\underline{\hat{\xi}}_{p,q})|\, \delta_{j,p}\, \delta_{k,q}\, \delta_{\ell,p}\, \delta_{m,q}.\end{aligned} \tag{2.26}$$

where $J_i(\hat{x}) := \det\left(DF_i(\hat{x})\right)$ with $DF_i(\hat{x})$ is the Jacobian matrix of $\underline{F}_i$.

From (2.26), we can easily deduce that

$$\int_{K_i} \varphi_{j,k}(\underline{x})\, \varphi_{\ell,m}(\underline{x}) \mathrm{d}\underline{x} \simeq \begin{cases} \hat{\omega}_{j,k}\, |J_i(\underline{\hat{\xi}}_{j,k})| \text{ if } \ell = j \text{ and } m = k, \\ \\ 0 \text{ otherwise,} \end{cases} \tag{2.27}$$

which obviously provides a diagonal mass-matrix.

A similar computation leads to the same conclusion in 3D.

Another and difficult question can be asked: Do we still keep the good order of approximation on distorted elements?

Actually, Ciarlet's criterion only applies to orthogonal elements (squares or cubes). So, the use of a mapping introduces a new difficulty to ensure the order of our approximation. This question will be addressed in the next chapter.

2.3 Triangles and Tetrahedra

Unlike tensor elements, the notions of spectral element and mass-lumping do not naturally coincide for other elements as triangles and tetrahedra. For such elements, mass-lumping cannot be obtained on the basis of classical interpolation points which lead to negative weights. Such weights lead, as we said above, to unconditionally unstable schemes. So, stable mass-lumping requires additional interpolation points for these elements, which induces some problems for their construction and their performance.

For this reason, we first present spectrally convergent elements, i.e. elements avoiding Runge phenomenon, based on Hesthaven's works [9, 15]. In a second part, we define mass-lumped elements introduced in [16, 17] for triangles up to third order and extended in [18] for higher-order tetrahedra and triangles.

2.3.1 Spectral Triangles and Tetrahedra

2.3.1.1 Finding Optimal Points

Natural Lagrange interpolation on triangles and tetrahedra is based on the P_r polynomial set defined, in dimension d, as

$$P_r = \left\{ v(\hat{\underline{x}}) = \sum_{\underline{j}=(j_1,\dots j_d),\ \sum_{\ell=1}^{d} j_\ell \le r} a_{\underline{j}} \prod_{k=1}^{d} \hat{x}_k^{j_k},\ a_{\underline{j}} \in \mathbb{R} \right\}. \tag{2.28}$$

Computation of quasi-optimal points (in terms of Runge phenomenon) for triangles and tetrahedra are based on an analogy with an optimization problem in electrostatics. This problems reads as follows:
Minimize the functional $W(\underline{x}_1, \dots, \underline{x}_{N_p})$ (which physically represents the electrostatic energy of N_p unit charges located at points $\{\underline{x}_1, \dots, \underline{x}_{N_p}\}$),

$$W(\underline{x}_1, \dots, \underline{x}_{N_p}) = \sum_{i=1}^{N_p} \left(\sum_{\ell=1}^{N_{\partial K}} \phi_\ell^L(\underline{x}_i) + \frac{1}{2} \sum_{j=1, j\neq i}^{N_p} \phi(\underline{x}_i, \underline{x}_j) \right), \tag{2.29}$$

where

$$\phi(\underline{x}_i, \underline{x}_j) = \frac{1}{|\underline{x}_i - \underline{x}_j|} \tag{2.30}$$

and

$$\phi_\ell^L(\underline{x}_i) = \int_{\gamma_\ell} \frac{\rho_\gamma}{|\underline{x} - \underline{x}_i|^2} \, \mathrm{d}\underline{x}. \tag{2.31}$$

N_p is the total number of points of interpolation, $N_{\partial K}$, the number of elementary components γ_ℓ of the boundary of the element (edges in 2D and faces in 3D), ρ_γ is a parameter of optimization on γ_ℓ.

Optimization is then made by solving numerically a N_p-body problem by integrating Newton's second law

$$\ddot{\underline{x}}_i + \sum_{\ell=1}^{N_{\partial K}} \nabla \phi_\ell^L(\underline{x}_i) + \sum_{j=1, j\neq i}^{N_p} \nabla \phi(\underline{x}_i, \underline{x}_j) + \varepsilon \dot{\underline{x}}_i = 0, \tag{2.32}$$

where ε is a positive constant which controls a dissipative term introduced for a computational purpose.

More details about this technique can be found in [9, 10, 15].

2.3.1.2 Optimal Points for the Unit Triangle and Tetrahedron

In Tables 2.5 and 2.6, we give the locations of the interior points for triangles and tetrahedra in barycentric coordinates. In these tables, r_m indicates the number of classes of points having an m-multiplicity (due to symmetry) in the element. For both elements, the Gauss-Lobatto points are used for the edges and do not appear in the tables. For this reason, we do not provide the points for the two first orders whose points are located on the edges. The number of interpolation points for P_r is equal to

- $\dfrac{(r+1)(r+2)}{2} = 3r + r_1 + 3r_3 + 6r_6$ for triangles,
- $\dfrac{(r+1)(r+2)(r+3)}{6} = 4 + 6(r-1) + r_1 + 4r_4 + 6r_6 + 12r_{12} + 24r_{24}$ for tetrahedra.

2.3.1.3 Computation of Basis Functions

The definition of the basis functions for these elements is slightly more complex than for tensor elements, for which basis functions can be constructed from products of 1D Lagrange polynomials, as mentioned in (2.19) and (2.20), or even triangle and tetrahedra with regularly spaced interpolation points. Actually, for these last

Table 2.5 Quasi-optimal interior points for triangles (to which summits and Gauss-Lobatto points on the edges (given in Tables 2.1 and 2.2) must be added)

r	r_1	r_3	r_6	λ_1	λ_2	λ_3
3	1			0.3333333333	0.3333333333	0.3333333333
4		1		0.2410021998	0.2410021998	0.5179956004
5		2		0.1591570023	0.1591570023	0.6816859954
				0.4099016620	0.4099016620	0.1801966760
6	1			0.3333333333	0.3333333333	0.3333333333
		1		0.1048904342	0.1048904342	0.7902191316
			1	0.3095036860	0.5582114022	0.1322849118
7		3		0.0666479037	0.0666479037	0.8667041924
				0.4474963910	0.4474963910	0.1050072180
				0.2606379453	0.2606379453	0.4787241094
			1	0.2328951264	0.6750593997	0.0920454739
8		3		0.0467325482	0.0467325482	0.9065349036
				0.2031909379	0.2031909379	0.5936181242
				0.3906323571	0.3906323571	0.2187352858
			2	0.3618069634	0.5544121321	0.0837809045
				0.1799524415	0.7523326932	0.0677148653
9	1			0.3333333333	0.3333333333	0.3333333333
		3		0.0354284515	0.0354284515	0.9291430970
				0.4641239296	0.4641239296	0.0717521408
				0.1632684184	0.1632684184	0.6734631632
			3	0.2965866112	0.6351919517	0.0682214371
				0.1437685751	0.8034472485	0.0527841764
				0.3225938344	0.4969468296	0.1804593360

elements, the basis functions are naturally defined by products of affine functions which are equations of straight lines or planes containing the interpolation points. In our case, we do not have such properties since the points are randomly spaced.

So, in order to get the basis functions, one must look for the coefficients of a complete polynomials of P_r, which implies to solve a linear system of dimension $(r+1)(r+2)/2$ for triangles and $(r+1)(r+2)(r+3)/6$ for tetrahedra. For high-order polynomials, this system is not well-conditioned and can be difficult to solve accurately. A palliative to this difficulty is the use of orthogonal basis functions of P_r, defined in [12] and used in [10]. Let us set $P_i^n = \widetilde{P}_i^{n,0}$, where $\widetilde{P}_i^{n,0}$ is the Jacobi polynomial defined by

$$\widetilde{P}_i^{(\ell,m)}(x) = \frac{(-1)^i}{2^i i!(1-x)^\ell(1+x)^m} \frac{\mathrm{d}^i}{\mathrm{d}x^i}((1-x)^\ell(1+x)^m(1-x^2)^i) \qquad (2.33)$$

Table 2.6 Quasi-optimal interior points for tetrahedra (to which summits and Gauss-Lobatto points on the edges (given in Tables 2.1 and 2.2) must be added)

r	r_1	r_4	r_6	r_{12}	r_{24}	λ_1	λ_2	λ_3	λ_4
3		1				0.3333333333	0.3333333333	0.3333333333	0.0000000000
4	1					0.2500000000	0.2500000000	0.2500000000	0.2500000000
				1		0.2371200168	0.2371200168	0.5257599664	0.0000000000
5		1				0.1834903473	0.1834903473	0.1834903473	0.4495289581
				2		0.1575181512	0.1575181512	0.6849636976	0.0000000000
						0.4105151510	0.4105151510	0.1789696980	0.0000000000
6		2				0.3333333333	0.3333333333	0.3333333333	0.0000000000
						0.1402705801	0.1402705801	0.1402705801	0.5791882597
			1			0.3542052583	0.3542052583	0.1457947417	0.1457947417
				1		0.1061169285	0.1061169285	0.7877661430	0.0000000000
					1	0.3097982151	0.5569099204	0.1332918645	0.0000000000
7		2				0.1144606542	0.1144606542	0.1144606542	0.6566180374
						0.2917002822	0.2917002822	0.2917002822	0.1248991534
				4		0.0660520784	0.0660520784	0.8678958432	0.0000000000
						0.4477725053	0.4477725053	0.1044549894	0.0000000000
						0.2604038024	0.2604038024	0.4791923952	0.0000000000
						0.1208429970	0.1208429970	0.4770203357	0.0000000000
					1	0.2325524777	0.6759625951	0.0914849272	0.0000000000
8	1					0.2500000000	0.2500000000	0.2500000000	0.2500000000
		1				0.0991203900	0.0991203900	0.0991203900	0.7026388300
			1			0.3920531037	0.3920531037	0.1079468963	0.1079468963
				5		0.0660520784	0.0660520784	0.8678958432	0.0000000000
						0.2033467796	0.2033467796	0.5933064408	0.0000000000
						0.3905496216	0.3905496216	0.2189007568	0.0000000000
						0.1047451941	0.1047451941	0.5581946462	0.2323149656
						0.2419418605	0.2419418605	0.4062097450	0.1099065340
					2	0.3617970895	0.5541643672	0.0840385433	0.0000000000
						0.1801396087	0.7519065566	0.0679538347	0.0000000000
9		3				0.3333333333	0.3333333333	0.3333333333	0.0000000000
						0.0823287303	0.0823287303	0.0823287303	0.7530138091
						0.2123055477	0.2123055477	0.2123055477	0.3630833569
				7		0.0355775717	0.0355775717	0.9288448566	0.0000000000
						0.4640303025	0.4640303025	0.0719393950	0.0000000000
						0.1633923069	0.1633923069	0.6732153862	0.0000000000
						0.0873980781	0.0873980781	0.6297057875	0.1954980564
						0.0916714679	0.0916714679	0.4819523024	0.3347047619
						0.2040338880	0.2040338880	0.4996292993	0.0923029247
						0.3483881173	0.3483881173	0.2075502723	0.0956734931
					3	0.2966333890	0.6349633653	0.0684032457	0.0000000000
						0.1439089974	0.8031490682	0.0529419344	0.0000000000
						0.3225890045	0.4968009397	0.1806100558	0.0000000000

These polynomials are orthogonal for the scalar product

$$(P, Q) = \int_{-1}^{1} (1-x)^{\ell}(1+x)^{m} P(x) Q(x) \mathrm{d}x. \tag{2.34}$$

We can now construct our orthogonal basis as follows

- For the unit triangle

$$\hat{T}_2 = \{(x_1, x_2) | \, x_1, \; x_2 \geq -1, \; x_1 + x_2 \leq -1\}, \tag{2.35}$$

we have

$$\varphi_{i,j} = P_i^0(a) P_j^{2i+1}(b)(1-b)^i, \quad i + j \leq r, \tag{2.36}$$

where $a = (2x_1 + x_2 + 1)/(1 - x_2)$ and $b = x_2$.

- For the unit tetrahedron

$$\hat{T}_3 = \{(x_1, x_2, x_3) | \, x_1, \; x_2, \; x_3 \geq -1, \; x_1 + x_2 + x_3 \leq -1\}, \tag{2.37}$$

we have

$$\begin{aligned} &\varphi_{i,j,k} = P_i^0(a) P_j^{2i+1}(b) P_k^{2i+2j+2}(c)(1-b)^i (1-c)^{i+j}, \\ &i + j + k \leq r, \end{aligned} \tag{2.38}$$

where $a = -(2x_1 + x_2 + x_3 + 2)/(x_2 + x_3)$, $b = (2x_2 + x_3 + 1)/(1 - x_3)$ and $c = x_3$.

Remarks:

1. a, b, c are related to x_1, x_2, x_3 by a mapping $\underline{F}_c$ from the unit cube $[-1, 1]^3$ (square $[-1, 1]^2$ in 2D) to our unit element (also called the Duffy's transform [19]). Actually, the functions $\varphi_{i,j,k} \circ \underline{F}_c^{-1}$ provide an orthogonal polynomial basis, as shown in [20].
2. Any other triangle or tetrahedron can be chosen for $\hat{T}_2$ and $\hat{T}_3$.
3. An easy way to get polynomials P_j^k is given by the following algorithm [21]

$$\begin{aligned} &P_0^k(x) = 1; \\ &P_1^k(x) = \frac{1}{2}[(k+2)x + k]; \\ &\forall j \geq 2, a_{j-2} = 2(j + k - 1)(j - 1)(2j + k), \\ &a_{j-1} = (2j + k - 1)[k^2 + (2j + k)(2j + k - 2)x], \\ &a_j = 2j(j + k)(2j + k - 2), \\ &P_j^k(x) = \frac{1}{a_j}(a_{j-1} P_{j-1}^k(x) - a_{j-2} P_{j-2}^k(x)). \end{aligned} \tag{2.39}$$

4. A Matlab procedure to compute the points is given in [10].

2.3.1.4 Extension to Triangles and Tetrahedra of Any Shape

In order to get an (H^1) extension of the basis functions to triangles and tetrahedra of any shape, we must first construct a mapping as follows for tetrahedra.

Let T be a tetrahedron of any shape and $\underline{F}_T$ the mapping such that $\underline{F}_T(\hat{T}_3) = T$. $\{a_1, a_2, a_3, a_4\}$ being the four vertices of T, we get

$$\underline{F}_T = \sum_{i=1}^{4} a_i \hat{\theta}_i, \tag{2.40}$$

where $\hat{\theta}_i$ are the basis functions of P_1 associated to $\hat{T}_3$, i.e.

$$\hat{\theta}_1 = \hat{x}_1 + \hat{x}_2 + \hat{x}_3 + 1, \quad \hat{\theta}_2 = \hat{x}_1 + 1, \quad \hat{\theta}_3 = \hat{x}_2 + 1, \quad \hat{\theta}_4 = \hat{x}_3 + 1$$

and as follows, for triangles:

Let T be a triangle of any shape and $\underline{F}_T$ the mapping such that $\underline{F}_T(\hat{T}_2) = T$. $\{a_1, a_2, a_3\}$ being the three vertices of T, we get

$$\underline{F}_T = \sum_{i=1}^{3} a_i \hat{\theta}_i, \tag{2.41}$$

where $\hat{\theta}_i$ are the basis functions of P_1 associated to $\hat{T}_2$, i.e.

$$\hat{\theta}_1 = \hat{x}_1 + \hat{x}_2 + 1, \quad \hat{\theta}_2 = \hat{x}_1 + 1, \quad \hat{\theta}_3 = \hat{x}_2 + 1.$$

2.3.2 *Mass-Lumped Triangles and Tetrahedra*

As we said, for triangles and tetrahedra, mass-lumping does not coincide with the spectral character of the elements. Actually, this difficulty arises from the fact that Gauss-Lobatto-like rules based on P_r interpolation points do exist, but they have some negative weights. The presence of such weights prohibits the use of these quadratures for transient wave equations since they lead to non positive approximations of the operator in space, which provides unconditionally unstable approximations.[4]

For instance, as shown in [7, 8, 16, 17], we get the following quadratures for P_2 and P_3 equilateral triangles[5]:

- For P_2, the points are the summits S_ℓ and the midpoints of the edges $M_\ell, \ell = 1 \ldots 3$ affected of weights $\omega_S = 0$ and $\omega_M = 1/6$, which is of course not acceptable.

[4] This difficulty is also troublesome for time-harmonic problems.

[5] P_1 is naturally mass-lumped by using the Trapezoidal rule for triangles and tetrahedra.

- For P_3, the points are the summits S_ℓ, $\ell = 1 \dots 3$, the center of the triangle G and the points of the edges $M_{12}(\theta)$, $M_{21}(\theta)$, $M_{13}(\theta)$, $M_{31}(\theta)$, $M_{23}(\theta)$, $M_{32}(\theta)$ such that $M_{\ell m}(\theta)$ is the barycenter of S_ℓ and S_m with the weights θ and $1-\theta$ (classically, $\theta = 1/3$). After some computations, we get $\theta = (3-\sqrt{3})/6$. The corresponding weights are then $\omega_S = -1/120$, $\omega_G = -9/40$, $\omega_M = 1/20$, which are also not acceptable.

In the same way, we have, as shown in [8], for the P_2 tetrahedron whose quadrature points are the summits S_ℓ, $\ell = 1 \dots 4$ and the midpoints of the edges M_ℓ, $\ell = 1 \dots 6$ affected of weights $\omega_S = -1/20$ and $\omega_M = 1/5$.

The palliative to this problem is to add degrees of freedom which implies to enrich the corresponding polynomial spaces P_r up to $P_{r'}, r' > r$. The new polynomial space $\check{P}_r$ is then such that $P_r \subset \check{P}_r \subset P_{r'}$. As shown in [17, 18], up to $r = 4$ for triangles, one must take $r' = r+1$ to get the appropriate quadrature rules with positive weights. In this case, the additional points represent about 50% of the initial points.

For $r > 4$ for triangles and for tetrahedra at any order, additional polynomials from P_{r+1} are not able to provide positive weights. One must take some other ones in $P_{r'}$, where $r' \geq r+2$. In this case, we multiply by about 2.5 points the initial number of points. At this stage, the increase of degrees of freedom seriously handicaps the method. Actually, besides the additional computational time induced by the important number of points, this number dramatically reduces the stability condition of the methods using these elements. Moreover, some experiments realized with continuous elements show that mass-lumped tetrahedra are less performant than classical ones.

For triangles, the polynomial space of interpolation is

$$\check{P}_r = P_r \oplus [b] P_{r'-3}, \tag{2.42}$$

where b is the so-called bubble function associated to the triangle and $[b] = \text{span}(b)$.

Remark: The bubble function of a triangle is defined as the product of its barycentric coordinates. For example, $b = x_1 x_2 (1 - x_1 - x_2)$ if we consider the triangle $\{(x_1, x_2) \,|\, x_1,\ x_2 \geq 0,\ x_1 + x_2 \leq 1\}$.

This definition shows that we have $3r + (r'-2)(r'-1)/2$ nodes which can be decomposed into

- $3r$ nodes on the edges,
- $(r'-2)(r'-1)/2$ interior nodes.

For tetrahedra, one must add polynomials related to the four faces as well as polynomials related to the interior of the tetrahedra. We get

$$\check{P}_r = P_r \oplus \sum_{i=1}^{4} [b_j] P_{r'-3} \oplus [\widetilde{b}] P_{r''-4}, \tag{2.43}$$

where $r' > r''$, $\widetilde{b}$ is the 3D bubble function and b_j is the bubble function related to the face opposite to the jth summit of the tetrahedron.

Remark: $\widetilde{b} = x_1x_2x_3(1 - x_1 - x_2 - x_3)$ for the tetrahedron $\{(x_1, x_2, x_3) \,|\, x_1,\ x_2,\ x_3 \geq 0,\ x_1 + x_2 + x_3 \leq 1\}$.

As for triangles, we have $6r - 2 + (r'' - 3)(r'' - 2)(r'' - 1)/6 + 2(r' - 2)(r' - 1)$ nodes which can be decomposed into

- $6r - 2$ nodes on the edges,
- $2(r' - 2)(r' - 1)$ on the faces,
- $(r'' - 3)(r'' - 2)(r'' - 1)/6$ interior nodes.

In order to construct the basis functions, one must determine the coefficients of a complete polynomial of $P_{r'}$. No orthogonal polynomial basis based on Jacobi polynomials was constructed for mass-lumped elements.

For such elements, Ciarlet's criterion reads as follows: In order to keep the approximation of finite element method of order r, one must use a quadrature rule at least exact for polynomials of P_N, where $N = r + r' - 2$. This criterion is fulfilled by the elements presented below.

In Figs. 2.5 and 2.6, we represent some mass-lumped triangles and tetrahedra. In Tables 2.7 and 2.8, we give the quadrature points and weights with their multiplicity for triangles and tetrahedra. The coordinates are given for the reference elements (i.e. with summits (0,0), (0,1) and (1,0) in 2D and (0,0,0), (1,0,0), (0,1,0) and (0,0,1) in 3D) for the closest points to the origin. Other points are obtained by central symmetry. Mass-lumped triangles for $r = 6$ and $r = 7$ can be found in [22].

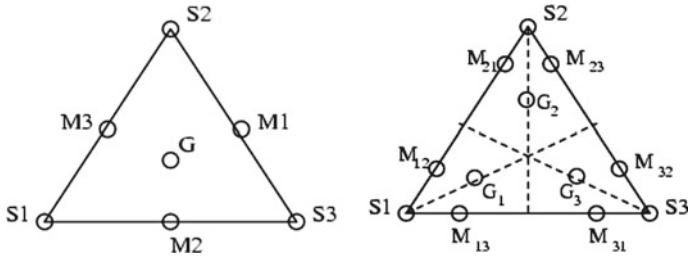

Fig. 2.5 The $\check{P}_2$ (*left*) and $\check{P}_3$ (*right*) triangular finite elements

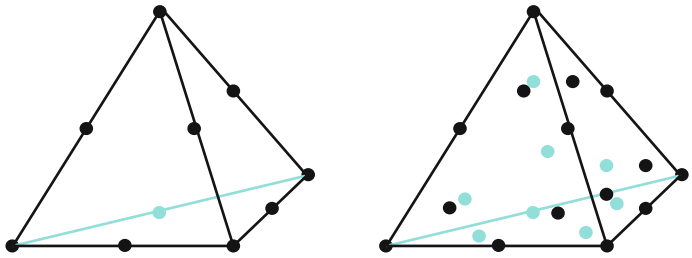

Fig. 2.6 The P_2 (*left*) and $\check{P}_2$ (*right*) tetrahedral elements

Table 2.7 Quadrature points and weights with their multiplicity for mass-lumped triangles

Element	Nodes	Mult.	Weights	Parameters
$r = r' = N = 1$	(0,0)	3	$\frac{1}{6}$	–
$r = 2, r' = 3,$ $N = 3$	(0,0)	3	$\frac{1}{40}$	–
	$\left(\frac{1}{2}, 0\right)$	3	$\frac{1}{15}$	–
	$\left(\frac{1}{3}, \frac{1}{3}\right)$	1	$\frac{9}{40}$	–
$r = 3, r' = 4,$ $N = 5$	(0,0)	3	$\frac{1}{90} - \frac{\sqrt{7}}{720}$	–
	(α,0)	6	$\frac{7}{720} - \frac{\sqrt{7}}{180}$	$\frac{1}{2} - \frac{\sqrt{441 - 84(7 - \sqrt{7})}}{42}$
	(β,β)	3	$\frac{49}{360} - \frac{7\sqrt{7}}{720}$	$\frac{1}{3}\left(1 - \frac{\sqrt{7}}{7}\right)$
$r = 4, r' = 5,$ $N = 7$	(0,0)	3	$\frac{1}{315}$	–
	$\left(\frac{1}{2}, 0\right)$	3	$\frac{4}{315}$	–
	(α,0)	6	$\frac{3}{280}$	$\frac{1}{2}\left(1 - \frac{\sqrt{3}}{3}\right)$
	(β_1,β_1)	3	$\frac{163}{2520} + \frac{47\sqrt{7}}{8820}$	$\frac{5 + \sqrt{7}}{18}$
	(β_2,β_2)	3	$\frac{163}{2520} - \frac{47\sqrt{7}}{8820}$	$\frac{5 - \sqrt{7}}{18}$
$r = 5, r' = 7,$ $N = 10$	(0,0)	3	0.709423970679E-03	–
	(α_1,0)	6	0.619056500367E-02	0.363298074154
	(α_2,0)	6	0.348057864050E-02	0.132264581633
	(β_1,β_1)	3	0.345043037728E-01	0.457836838079
	(β_2,β_2)	3	0.459012376308E-01	0.256859107620
	(β_2,β_2)	3	0.116261354596E-01	0.575276844114
	(γ,δ)	6	0.272785759700E-01	γ =0.781925836255
				δ =0.221001218760

Table 2.8 Quadrature points and weights with their multiplicity for mass-lumped tetrahedra

Element	Nodes	Mult.	Weights	Parameters
$r = r' = 1$ $r'' = N = 1$	(0,0,0)	4	$\frac{1}{24}$	–
$r = 2,$ $r' = 4,$ $r'' = N = 4$	(0,0,0)	4	$\frac{13 - 3\sqrt{13}}{10080}$	–
	$\left(\frac{1}{2}, 0, 0\right)$	6	$\frac{4 - \sqrt{13}}{315}$	–
	$(\alpha, \alpha, 0)$	12	$\frac{29 + 17\sqrt{13}}{10080}$	$\frac{7 - \sqrt{13}}{18}$
	$\left(\frac{1}{4}, \frac{1}{4}, \frac{1}{4}\right)$	1	$\frac{16}{315}$	–
$r = 3,$ $r' = 6,$ $r'' = 5,$ $N = 7$	(0,0,0)	4	0.214360866805E-03	–
	$(\alpha, 0, 0)$	12	0.826817951780E-03	0.292829404767
	$(\beta_1, \beta_1, 0)$	12	0.184017790419E-02	0.197286228026
	$(\beta_2, \beta_2, 0)$	12	0.183132432925E-02	0.425646124314
	(γ, γ, γ)	4	0.754246890465E-02	0.950377585839E-01
	$\left(\delta, \delta, \frac{1}{2} - \delta\right)$	4	0.136099175597E-01	0.125246236258

2.4 Purely 3D Elements

It seems obvious that hexahedra hold interesting properties which enable us to get both spectral and mass-lumped elements. Unfortunately, it is very difficult to produce a purely hexahedral mesh for complex geometries.[6] A palliative to this difficulty is to construct hybrid meshes, containing tetrahedra and (mainly) hexahedra. In order to hybridize these two kinds of elements, it is useful to use pyramids and even wedges to stick together the different shapes.[7]

[6] Unless by splitting tetrahedra into four hexahedra, which provides a very distorted mesh. This distortion leads to very bad performance in terms of accuracy and stability.

[7] One must keep in mind that, besides the fact that the faces of tetrahedra lean on three edges and those of hexahedra on four, the first faces are plane while the second ones are not always plane. Thereby, even by sticking the edges of two triangular faces of two tetrahedra to the four edges of the quadrangular face of a an hexahedron, we get overlapping or underlapping of the elements. For this reason, pyramids and wedge are useful interfaces between tetrahedra and hexahedra.

2.4.1 Wedges

H^1-wedges are easy to construct. We first define a unit prism $\hat{W}$ by a tensor product of an unit triangle and a 1D spectral element of the same order (one can also mix the orders) which provides a regular element with plane faces. The 1D element is in the $\hat{x}_3$-direction. In other words, the polynomial space of order r associated to the unit prism is

$$P_r(\hat{x}_1, \hat{x}_2) \otimes P_{r'}(\hat{x}_3), \tag{2.44}$$

where $P_r(\hat{x}_1, \hat{x}_2)$ is the polynomial space on the unit triangle and $P_{r'}(\hat{x}_3)$ the 1D polynomial space in variable $\hat{x}_3$. Its dimension is $(r+1)(r+2)(r'+1)/2$.

The basis functions are the Cartesian product of the set of the basis functions on the unit triangle and the basis functions on $[0, 1]$. In general, one takes $r' = r$.

In a second step, in order to construct a wedge W of any shape (with straight edges) we define a transform $\underline{F}^w$ based on the six Q_1 basis functions of the unit prism, i.e.,

$$\hat{p}_1(\hat{x}_1, \hat{x}_2, \hat{x}_3) = (1 - \hat{x}_1 + \hat{x}_2)(1 - \hat{x}_3),\ \hat{p}_2(\hat{x}_1, \hat{x}_2, \hat{x}_3) = \hat{x}_1(1 - \hat{x}_3),$$

$$\hat{p}_3(\hat{x}_1, \hat{x}_2, \hat{x}_3) = \hat{x}_2(1 - \hat{x}_3),\ \hat{p}_4(\hat{x}_1, \hat{x}_2, \hat{x}_3) = (1 - \hat{x}_1 + \hat{x}_2)\hat{x}_3,$$

$$\hat{p}_5(\hat{x}_1, \hat{x}_2, \hat{x}_3) = \hat{x}_1\hat{x}_3,\ \hat{p}_6(\hat{x}_1, \hat{x}_2, \hat{x}_3) = \hat{x}_2\hat{x}_3,$$

which reads

$$\underline{F}_i^w(\hat{x}_1, \hat{x}_2, \hat{x}_3) = \sum_{j=1}^{6} \underline{a}_j \hat{p}_j(\hat{x}_1, \hat{x}_2, \hat{x}_3), \tag{2.45}$$

where $\underline{a}_j$ are the summits of a given wedge $((\underline{a}_1, \underline{a}_2, \underline{a}_3)$ and $(\underline{a}_4, \underline{a}_5, \underline{a}_6)$ respectively being the summits of the two triangular faces of the wedge).

As for other elements, basis functions p_i on W are defined by

$$p_i \circ \underline{F}_i^w = \hat{p}_i.$$

Remark: One can use higher-order basis functions to get curved edges.

2.4.2 Pyramids

Constructing nodal pyramidal finite elements is not an obvious problem since its direct definition cannot be based on a polynomial space if we want to preserve the conformity of pyramids with other elements[8] [23]. For this reason, Bedrosian

[8] More precisely, the use of polynomial functions does not keep the plane character of the triangular faces when one transforms a reference pyramid into a pyramid of any shape.

introduced a space of rational functions and constructed rational basis functions of order 1 and 2 [23]. However, the quadrilateral face had no node at its center, which avoids the conformity with hexahedra. Zgainski et al. [24] added a center node which was not optimal. Graglia et al. [25] introduced a new basis function at the center of the face which provides an optimal element. Chatzi and Preparata [26] were the first to introduce a basis of any order. Unfortunately, their basis are consistent up to third order.

An important step, based on the *hp* approach [27, 28], was realized by Karniadakis, Sherwin et al. and Warburton [20, 29–31] who constructed consistent pyramidal finite elements of any order with an optimal error for first-order mapping.

In the following, we provide a way to construct pyramidal finite elements of any order following [32] (and close to that introduced by Karniadakis et al. and Zaglmayr [33]) which seems to have optimal error estimates for high-order mappings.

2.4.2.1 The Space of Rational Functions on the Unit Pyramid

The main difficulty to construct a pyramidal finite element is the definition of the space to which belong the functions. Let us first define the space $\mathscr{P}_r$ corresponding to the unit pyramid $\hat{\Pi}$, i.e. the (symmetric) pyramid whose summits are $\underline{\hat{a}}_1 = (-1,-1,0)$, $\underline{\hat{a}}_2 = (1,-1,0)$, $\underline{\hat{a}}_3 = (1,1,0)$, $\underline{\hat{a}}_4 = (-1,1,0)$, $\underline{\hat{a}}_5 = (0,0,1)$ (Fig. 2.7)

$$\mathscr{P}_r = P_r(\hat{x}_1,\hat{x}_2,\hat{x}_3) \oplus \sum_{k=0}^{r-1} \left(\frac{\hat{x}_1\hat{x}_2}{1-\hat{x}_3}\right)^{r-k} P_k(\hat{x}_1,\hat{x}_2), \tag{2.46}$$

where $P_k(\hat{x}_1,\hat{x}_2)$ and $P_r(\hat{x}_1,\hat{x}_2,\hat{x}_3)$ are the two polynomial spaces introduced in (2.28) for $d=2$ and $d=3$. After some computations (using the formula $\sum_{k=1}^{n} k^2 =$

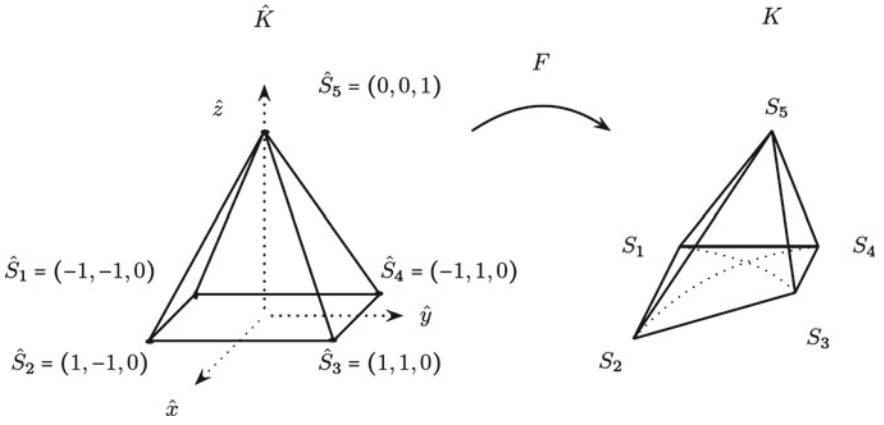

Fig. 2.7 First-order mapping for a pyramid

$n(n+1)(n+2)/6)$, one can check that

$$\dim \mathscr{P}_r = \frac{1}{6}(r+1)(r+2)(2r+3).$$

Remark: We have $\dim P_r < \dim \mathscr{P}_r < \dim Q_r$.

2.4.2.2 Construction of Pyramids of Any Shape

In a second step, we construct a pyramid Π of any shape (with straight edges) by using the mapping based on the five shape functions $\left(\hat{p}_i\right)_{i=1}^{5}$ of $\mathscr{P}_1$ such that $\hat{p}_i(\underline{\hat{a}}_j) = \delta_{ij}$, δ_{ij} being the Kronecker symbol (Fig. 2.7). This mapping reads

$$\underline{F}^{\pi}(\hat{x}_1, \hat{x}_2, \hat{x}_3) = \sum_{j=1}^{5} \underline{a}_j \hat{p}_j(\hat{x}_1, \hat{x}_2, \hat{x}_3), \tag{2.47}$$

where $\left(\underline{a}_i\right)_{i=1}^{5}$ are the summits of Π and

$$\begin{cases} \hat{p}_1(\hat{x}_1, \hat{x}_2, \hat{x}_3) = \dfrac{1}{4}\left(1 - \hat{x}_1 - \hat{x}_2 - \hat{x}_3 + \dfrac{\hat{x}_1\hat{x}_2}{1-\hat{x}_3}\right), \\ \hat{p}_2(\hat{x}_1, \hat{x}_2, \hat{x}_3) = \dfrac{1}{4}\left(1 + \hat{x}_1 - \hat{x}_2 - \hat{x}_3 - \dfrac{\hat{x}_1\hat{x}_2}{1-\hat{x}_3}\right), \\ \hat{p}_3(\hat{x}_1, \hat{x}_2, \hat{x}_3) = \dfrac{1}{4}\left(1 + \hat{x}_1 + \hat{x}_2 - \hat{x}_3 + \dfrac{\hat{x}_1\hat{x}_2}{1-\hat{x}_3}\right), \\ \hat{p}_4(\hat{x}_1, \hat{x}_2, \hat{x}_3) = \dfrac{1}{4}\left(1 - \hat{x}_1 + \hat{x}_2 - \hat{x}_3 - \dfrac{\hat{x}_1\hat{x}_2}{1-\hat{x}_3}\right), \\ \hat{p}_5(\hat{x}_1, \hat{x}_2, \hat{x}_3) = \hat{x}_3. \end{cases} \tag{2.48}$$

$\underline{F}^{\pi}$ can also be written on the canonical basis of $\mathscr{P}_1$ as follows:

$$\begin{aligned} \underline{F}^{\pi}(\hat{x}_1, \hat{x}_2, \hat{x}_3) = \frac{1}{4}\Big[&(\underline{a}_1 + \underline{a}_2 + \underline{a}_3 + \underline{a}_4) \\ &+\hat{x}_1(-\underline{a}_1 + \underline{a}_2 + \underline{a}_3 - \underline{a}_4) \\ &+\hat{x}_2(-\underline{a}_1 - \underline{a}_2 + \underline{a}_3 + \underline{a}_4) \\ &+\hat{x}_3(4\underline{a}_5 - \underline{a}_1 - \underline{a}_2 - \underline{a}_3 - \underline{a}_4) \\ &+\frac{\hat{x}_1\hat{x}_2}{1-\hat{x}_3}(\underline{a}_1 - \underline{a}_2 + \underline{a}_3 - \underline{a}_4)\Big]. \end{aligned} \tag{2.49}$$

Here also, we have, for any basis function p_i on Π,

$$p_i \circ \underline{F}_i^{\pi} = \hat{p}_i.$$

Remarks:

1. Pyramids are not convenient for they have the drawback of hexahedra since $\underline{F}^{\pi}$ is not linear, which implies a storage of the Jacobian and the Jacobian matrix at each point of interpolation and the drawback of tetrahedra since they are not based on tensor products, which makes it difficult, even impossible, to construct mass-lumped pyramids. A palliative to this problem is the use of the Duffy's transform [19] which enables us to map a cube to a pyramid. The way to get (discontinuous) mass-lumped pyramids is to map the unit cube with Gauss points defined in Sect. 2.2.2 to a pyramid. The corresponding method of quadrature introduced by Radau [34] is quoted in [35] for triangles and was applied to pyramids [36].
2. Another feature of Duffy's transform is to provide a simple definition of $\mathscr{P}_r$. This space is merely the transform of the following polynomial space

$$C_r = \text{span}\{x^i y^j (1-z)^k, \quad 0 \le i, j \le k \le r\} \tag{2.50}$$

   from the unit cube $[0, 1]^3$ to $\hat{\Pi}$.
3. One can use higher-order basis functions to get pyramids with curved edges.

2.4.2.3 Construction of Higher Order Basis Functions

In order to ensure the continuity between pyramids and the other types of elements (and also to simplify the computation for discontinuous methods), the nodes on the four triangular faces of $\hat{\Pi}$ coincide with Hesthaven's points on the faces of a tetrahedron and the nodes of the base of $\hat{\Pi}$ are located at the Gauss-Lobatto coordinates. Interior nodes (if any) are added by taken into account symmetry (Fig. 2.8). Let us call $\left(\underline{\hat{c}}_i\right)_{i=1}^{\dim \mathscr{P}_r}$ these nodes.

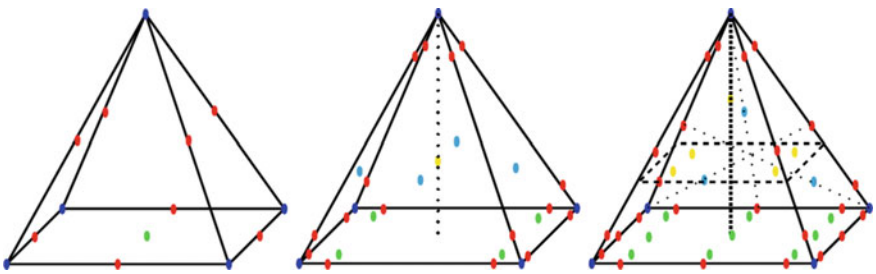

Fig. 2.8 Nodes for pyramids of order 2, 3, 4

For $\mathscr{P}_2$, we have $\dim \mathscr{P}_2 = 14$ and its canonical basis $\left(p_i^c\right)_{i=1}^{14}$ is

$$\{1, \hat{x}_1, \hat{x}_2, \hat{x}_3, \hat{x}_1\hat{x}_2, \hat{x}_1\hat{x}_3, \hat{x}_2\hat{x}_3, \hat{x}_1^2, \hat{x}_2^2, \hat{x}_3^2, \hat{r}, \hat{x}_1\hat{r}, \hat{x}_2\hat{r}, \hat{r}^2\},$$

where $\hat{r} = \hat{x}_1\hat{x}_2/(1-\hat{x}_3)$.

So, a basis functions of $\hat{p}_i \in \mathscr{P}_2$ such that $\hat{p}_i(\underline{\hat{c}}_j) = \delta_{ij}$ can be decomposed as

$$\hat{p}_i = \sum_{j=1}^{14} \lambda_j^i p_j^c, \quad \lambda_j^i \in \mathbb{R}. \tag{2.51}$$

A natural way to compute these basis functions is to solve, for each $i = 1 \dots 14$ the following (Vandermonde-like) linear systems in λ_j^i:

$$\sum_{j=1}^{14} \lambda_j^i p_j^c(\underline{\hat{c}}_k) = \delta_{ik}, \quad \forall k = 1 \dots 14. \tag{2.52}$$

Unfortunately, as for tetrahedra, this system is ill-conditioned for high orders (Fig. 2.9). A palliative to this problem is to use an extension of the orthogonal basis introduced in (2.38). This basis is given by

$$\begin{aligned} &\varphi_{i,j,k} = P_i^0(2a-1)P_j^0(2b-1)(1-c)^{\max(i,j)}P_k^{2\max(i,j)+2}(2c-1), \\ &0 \le i, j \le r, 0 \le k \le r - \max(i,j), \end{aligned} \tag{2.53}$$

where $a = (\hat{x}_1 - \hat{x}_3 + 1)/2(1-\hat{x}_3)$, $b = (\hat{x}_2 - \hat{x}_3 + 1)/2(1-\hat{x}_3)$, $c = \hat{x}_3$ and P_k^2 is defined as in (2.39).

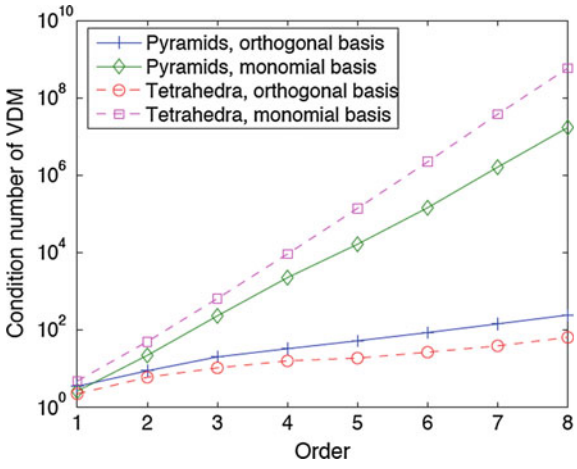

Fig. 2.9 Condition number of the linear systems providing nodal basis functions for tetrahedra and pyramids

Remark: An orthogonal basis can be used to define modal finite elements, which provide mass-lumping in discontinuous Galerkin methods [37].

2.5 Tetrahedral and Triangular Edge Elements

2.5.1 Mixed Formulation

Edge elements belong to the family of mixed finite elements which seem to have been derived from the Hellinger-Reissner principle for elasticity by Fraeijs de Veubeke [38]. This principle is to split a second order PDE system into two first order equations and to use different finite element approximations for each equation. First used for elastics, this approach was studied for the 2D harmonic problem [39] and eventual other problems and extended for 3D elements in [40]. For instance, the harmonic problem

$$-\Delta u = f \tag{2.54}$$

is replaced by

$$\begin{aligned} -\nabla \cdot \underline{q} &= f, \\ \underline{q} &= \nabla u. \end{aligned} \tag{2.55}$$

In a second step, u is sought in L^2 and $\underline{q}$ in $H(div)$. One can notice that, in such formulation, only one variable $\underline{q}$ keeps its physical character (normal continuity), the (continuous) character of the second one being weakened. Although classical, we shall see later that this choice is not unique.

An important extension of this approach for Maxwell's equations was given by Nédélec [40, 41] who constructed two families of edge elements, i.e. finite elements which belong to $H(curl)$ and then keep the important tangential continuity of the electric field.

Despite the anteriority of $H(div)$-conform elements, we first describe the $H(curl)$-conform elements which are more suited to wave phenomena. In the following, we just give a description of these elements. A exhaustive study of their properties can be found in [42].

2.5.2 A First Family

We describe in this section the first family of edge elements defined in [40], which is the most popular and which is also the most suited to Maxwell's equations.

2.5.2.1 The Polynomial Space

Let us first define the polynomial space $\mathscr{R}_r$ involved for the unit tetrahedron $\hat{T}_3$ defined at (2.37). We have

$$\mathscr{R}_r = (P_{r-1})^3 \oplus \underline{S}_r, \tag{2.56}$$

where

$$\underline{S}_r = \left\{ \underline{p} \in (\widetilde{P}_r)^3 \text{ such that } \underline{\hat{x}} \cdot \underline{p} = 0,\ \underline{x} \in \mathbb{R}^3 \right\}, \tag{2.57}$$

with

$$\widetilde{P}_r = \left\{ \sum_{i+j+k=r} a_{i,j,k}\, \hat{x}_1^i\, \hat{x}_2^j\, \hat{x}_3^k, \quad a_{i,j,k} \in \mathbb{R} \right\} \tag{2.58}$$

is the space of homogeneous polynomials of order r.

Obviously, $\dim (P_{r-1})^3 = r(r+1)(r+2)/2$. On the other hand, it is easy to see that $\widetilde{P}_{r+1} = \text{span}\{\underline{\hat{x}} \cdot \underline{p},\ \underline{p} \in (\widetilde{P}_r)^3\}$ and $\dim \widetilde{P}_r = (r+1)(r+2)/2$. So, $\dim \underline{S}_r = \dim (\widetilde{P}_r)^3 - \dim \widetilde{P}_{r+1} = 3(r+1)(r+2)/2 - (r+2)(r+3)/2 = r(r+2)$. Finally

$$\dim \mathscr{R}_r = \frac{1}{2} r(r+2)(r+3). \tag{2.59}$$

An important issue is the construction of $\underline{S}_r$ which is not natural because of the constraint $\underline{\hat{x}} \cdot \underline{p} = 0$. In [43], $\underline{S}_r$ is characterized as follows

$$\underline{S}_r = \text{span}\{\underline{V}_1, \underline{V}_2, \underline{V}_3\}, \tag{2.60}$$

with

$$\underline{V}_1 = \begin{pmatrix} \hat{x}_1^{m-1}\, \hat{x}_2^n\, \hat{x}_3^{r-m-n+1} \\ 0 \\ -\hat{x}_1^m\, \hat{x}_2^n\, \hat{x}_3^{r-m-n} \end{pmatrix}, \quad 0 \le m+n \le r, m \ne 0, n \ne r, \tag{2.61}$$

$$\underline{V}_2 = \begin{pmatrix} 0 \\ \hat{x}_1^m\, \hat{x}_2^{n-1}\, \hat{x}_3^{r-m-n+1} \\ -\hat{x}_1^m\, \hat{x}_2^n\, \hat{x}_3^{r-m-n} \end{pmatrix}, \quad 0 \le m+n \le r, m \ne r, n \ne 0, \tag{2.62}$$

$$\underline{V}_3 = \begin{pmatrix} \hat{x}_1^{m-1}\, \hat{x}_2^n \\ -\hat{x}_1^m\, \hat{x}_2^{n-1} \\ 0 \end{pmatrix}, \quad m+n = r+1, m \ne 0, n \ne 0. \tag{2.63}$$

Thanks to (2.60)–(2.63), one can construct the basis functions of the method. In order to get a better conditioned system, one can use an orthogonal basis of $(P_{r-1})^3$ and even express (2.61)–(2.63) in terms of orthogonal polynomials.

2.5.2.2 The Degrees of Freedom

In order to construct the basis functions, one must define the degrees of freedom for our method. In our case, these degrees of freedom are not values of the functions at some interpolation points, but tangent and volume momenta which a priori easier define the tangential continuity of the solution.

Following [40], we have three types of degrees of freedom:

1. $6r$ integrals on the edges defined by

$$\int_e \underline{u} \cdot \underline{t} q \, \mathrm{d}\hat{\sigma}, \quad \forall q \in P_{r-1},$$

   where $\underline{t}$ is an unit vector along an edge $e \in \hat{T}_3$.
2. $4r(r-1)$ integrals on the faces defined by

$$\int_f (\underline{u} \times \underline{n}) \cdot \underline{q} \, \mathrm{d}\hat{\underline{\gamma}}, \quad \forall \underline{q} \in (P_{r-2})^2,$$

   where $\underline{n}$ is the unit vector normal to a face $f \in \hat{T}_3$.
3. $r(r-1)(r-2)/2$ integrals in $\hat{T}_3$ defined by

$$\int_{\hat{T}_3} \underline{u} \cdot \underline{q} \, \mathrm{d}\hat{\underline{x}}, \quad \forall \underline{q} \in (P_{r-3})^3.$$

One can easily check that we have $r(r+2)(r+3)/2$ degrees of freedom. One can find the two first order basis functions in [40] and the third order in [44].

2.5.2.3 Extension to Any Tetrahedron

The extension to any tetrahedron of these functions must take into account the tangential continuity of the solution all over a mesh.

If $\hat{B}$ and B are the sets of basis functions on $\hat{T}_3$ and T respectively, for $\hat{\underline{\varphi}} \in \hat{B}$ and $\underline{\varphi} \in B$, the classical transform $\underline{\varphi} \circ \underline{F}_T = \hat{\underline{\varphi}}$ (used for H^1 functions which are globally continuous) would not ensure the tangential continuity. For this reason, this transform is replaced by the $H(curl)$-conform transform which ensures the tangential continuity

$$\underline{\varphi} \circ \underline{F}_T = DF_T^{-T} \hat{\underline{\varphi}}, \tag{2.64}$$

where DF_T^{-T} is the inverse of the transposed Jacobian matrix of $\underline{F}_T$ defined in (2.40).

Remarks:

1. DF_T is a constant matrix. One can use higher-order basis functions to define $\underline{F}_T$ in order to construct elements with curved faces by using the Gordon-Hall transform [13, 14]. In this case, DF_T is no longer constant.
2. Combined with the first family of $H(div)$-conform finite elements, this family provides a spurious-free approximation of Maxwell's equations.
3. The definition of the degrees of freedom seems to indicate that we have a family of modal elements. Actually, one can construct basis functions by using r vector-valued functions tangent to each edge, $r(r-1)$ functions tangent to each face and $r(r-1)(r-2)/2$ functions inside the tetrahedron. Then the $H(curl)$-conform transform would ensure the tangential continuity. This second definition is very useful for mass-lumping, as described below.

2.5.2.4 Triangles

As for tetrahedra, the edge element can be defined in a modal way on the unit triangle $\hat{T}_2$ defined at (2.35) by using the following degrees of freedom:

1. $3r$ integrals on the edges defined by

$$\int_e \underline{u} \cdot \underline{t} q \, \mathrm{d}\hat{\sigma}, \quad \forall q \in P_{r-1},$$

   where $\underline{t}$ is the unit vector along an edge $e \in \hat{T}_2$.
2. $r(r-1)$ integrals in $\hat{T}_2$ defined by

$$\int_{\hat{T}_2} \underline{u} \cdot \underline{q} \, \mathrm{d}\underline{\hat{x}}, \quad \forall \underline{q} \in (P_{r-2})^2,$$

or in a nodal way, by using pointwise values of r vector-valued functions tangent to each edge and $r(r-1)$ interior vector-valued functions collinear to the canonical basis of $\mathbb{R}^2$.

The corresponding polynomial space $\mathscr{R}_r^T$ is defined, as for tetrahedra, by

$$\mathscr{R}_r^T = (P_{r-1})^2 \oplus \underline{S}_r^T, \tag{2.65}$$

where

$$\underline{S}_r^T = \left\{ \underline{p} \in (\widetilde{P}_r)^2 \text{ such that } \underline{\hat{x}} \cdot \underline{p} = 0, \ \underline{x} \in \mathbb{R}^2 \right\}. \tag{2.66}$$

As for tetrahedra, one can show that $\dim \underline{S}_r^T = r$ and $\dim \mathscr{R}_r^T = r(r+2) = 3r + r(r-1)$.

More explicitly, we can write

$$\underline{S}_r^T = \text{span}\{\underline{V}\}, \tag{2.67}$$

with

$$\underline{V} = \begin{pmatrix} \hat{x}_1^{m-1}\,\hat{x}_2^n \\ -\hat{x}_1^m\,\hat{x}_2^{n-1} \end{pmatrix}, \quad m+n = r+1, m \neq 0, n \neq 0. \tag{2.68}$$

Extension to any triangle is made by using (2.64), where $\underline{F}_T$ is then defined as in (2.41).

2.5.3 A Second Family

The second family of edge elements introduced by Nédélec [41] is composed of polynomials of $(P_r)^3$. In order to define the corresponding degrees of freedom, let us first introduce the polynomial spaces

$$\mathscr{D}_r^d = (P_{r-1})^d \oplus \underline{x}\,\widetilde{P}_{r-1}, \tag{2.69}$$

where d is the dimension of space and $\widetilde{P}_r$ is defined as in Sect. 2.5.2. We have $\dim \mathscr{D}_r^2 = r(r+2)$ and $\dim \mathscr{D}_r^3 = r(r+1)(r+3)/2$.

We can now define the degrees of freedom for this family:

1. $6(r+1)$ integrals on the edges defined by

$$\int_e \underline{u} \cdot \underline{t} q \, \mathrm{d}\hat{\sigma}, \quad \forall q \in P_r(e),$$

where $\underline{t}$ is the unit vector along an edge $e \in \hat{T}_3$.

2. $4(r^2-1)$ integrals on the faces defined by

$$\int_f \underline{u} \cdot \underline{q} \, \mathrm{d}\hat{\underline{\gamma}}, \quad \forall \underline{q} \in \mathscr{D}_{r-1}^2(f), \text{ for any face } f \text{ of } \hat{T}_3.$$

2. $(r^2-1)(r-2)/2$ integrals in $\hat{T}_3$ defined by

$$\int_{\hat{T}_3} \underline{u} \cdot \underline{q} \, \mathrm{d}\underline{\hat{x}}, \quad \forall \underline{q} \in \mathscr{D}_{r-2}^3.$$

We get $6(r+1) + 4(r^2-1) + (r^2-1)(r-2)/2 = \dim(P_r)^3$.

Extension to any element T is made in the same way as the first family.

It seems that this family does not provide a spurious-free approximation of Maxwell's equations.

Remarks:

1. The above degrees of freedom can be replaced by values at Hesthaven's points of three vector-valued functions. These functions are tangent to the edges at the summits, tangent to the edge and to the two faces (and orthogonal to the edge) for points located on an edge, tangent to a face and normal to this face (and orthogonal to each other) for points located on a face and collinear to the canonical basis vectors for an interior point (cf. Fig. 2.10).
2. This element was also suggested by Mur et al. [45].

2.5.3.1 Triangles

For the unit triangle $\hat{T}_2$, the polynomial space is $(P_r)^2$ and degrees of freedom are:

1. $3(r+1)$ integrals on the edges defined by

$$\int_e \underline{u} \cdot \underline{t} q \, \mathrm{d}\hat{\sigma}, \quad \forall q \in P_r(e),$$

   where $\underline{t}$ is the unit vector along an edge $e \in \hat{T}_2$.
2. (r^2-1) integrals inside the triangle defined by

$$\int_{\hat{T}_2} \underline{u} \cdot \underline{q} \, \mathrm{d}\underline{\hat{x}}, \quad \forall \underline{q} \in \mathscr{D}^2_{r-1}.$$

In a nodal way, the degrees of freedom are the values of $6r$ vector-valued functions tangent or orthogonal to each edge and $(r-1)(r-2)$ interior vector-valued functions collinear to the canonical basis of $\mathbb{R}^2$ at Hesthaven's points.

Obviously, we get $3(r+1) + (r^2-1) = 6r + (r-1)(r-2) = \dim(P_r)^2$.

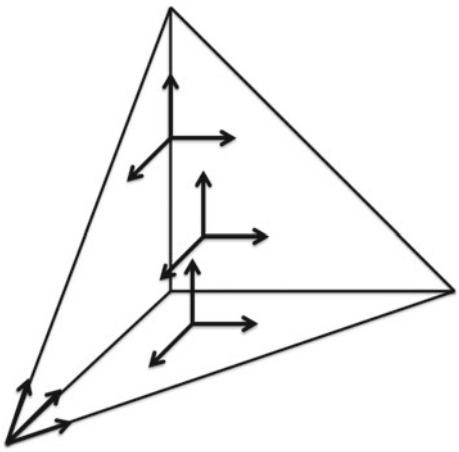

Fig. 2.10 The locations of the degrees of freedom for the second family of edge elements

2.5.4 Tetrahedral Mass-Lumped Edge Elements

2.5.4.1 The First-Order Element

Let (S_1, S_2, S_3, S_4) be the vertices of $\hat{T}_3$ and $(\lambda_1, \lambda_2, \lambda_3, \lambda_4)$ the corresponding barycentric coordinates. An edge is defined by its ends and each face is assigned to the index of its opposite vertex. So, a face Φ_j is such that $S_j \notin \Phi_j$. At each midpoint M_{pq} of an edge S_pS_q, we define the three unit vectors $(\underline{e}_{pq,1}, \underline{e}_{pq,2}, \underline{e}_{pq,3})$ such that $\underline{e}_{pq,1}$ is collinear to S_pS_q, and $\underline{e}_{pq,2}, \underline{e}_{pq,3}$ are the two vectors orthogonal to $\underline{e}_{pq,1}$ and parallel to the two faces containing S_pS_q. The degrees of freedom are the three components of a function at the point M_{pq} in this local basis, for each edge of the tetrahedron T (Fig. 2.11). So, we have 18 degrees of freedom (instead of 6 for the regular first family).

Now, let us set $I = \{(\{\ell, m\}, n)$ such that $(\ell, m, n) \in \{1, 2, 3, 4\}^3, \ell \neq m, n \neq \ell, n \neq m\}$. We can define the following spaces of polynomial vector-valued functions

$$\mathscr{S}_1 = \{\underline{u}(\underline{\hat{x}}) = \underline{a} \times \underline{\hat{x}} + \underline{b},\ (\underline{a}, \underline{b}) \in \mathbb{R}^3 \times \mathbb{R}^3\}, \tag{2.70}$$

$$\widetilde{\mathscr{S}_1} = \mathscr{S}_1 \oplus \{\underline{w}^n_{\ell m}\}_{(\{\ell,m\},n)\in I}, \tag{2.71}$$

where

$$\underline{w}^n_{\ell m} = \lambda_\ell \lambda_m \nabla \lambda_n, \tag{2.72}$$

and ∇ is the gradient versus $\underline{\hat{x}}$.

Let $\underline{\nu}_j$ be the unit outward normal to a face $\Phi_j = S_\ell S_m S_n$. If we set

$$\nabla_j \underline{w} = \underline{\nu}_j \times ((\nabla \underline{w})_{|\Phi_j} \times \underline{\nu}_j), \tag{2.73}$$

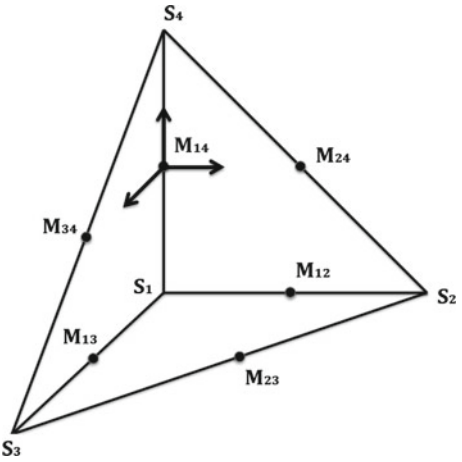

Fig. 2.11 The locations of the degrees of freedom and the three degrees of freedom at the point M_{14} for $\widetilde{\mathscr{S}_1}$ (see (2.71))

which is actually the surface gradient of $\underline{w}$ on Φ_j, we have

$$\underline{\nu}_j \times ((\underline{w}^n_{\ell m})_{|_{\Phi_j}} \times \underline{\nu}_j) = \underline{t}^n_{\ell m} = \lambda_\ell \lambda_m \nabla_j \lambda_j. \tag{2.74}$$

Let

$$\mathscr{R}_1(\Phi_j) = \{\underline{\nu}_j \times (\underline{u}_{|_{\Phi_j}} \times \underline{\nu}_j),\ \underline{u} \in \mathscr{S}_1\} \tag{2.75}$$

be the space of the tangential traces of functions of $\mathscr{S}_1$ and

$$\widetilde{\mathscr{R}}_1(\Phi_j) = \mathscr{R}_1(\Phi_j) \oplus \{\underline{t}^n_{\ell m}, \underline{t}^m_{n\ell}, \underline{t}^\ell_{mn}\}. \tag{2.76}$$

Equation (2.74) implies that $\widetilde{\mathscr{R}}_1(\Phi_j)$ is the space of the tangential traces of functions of $\widetilde{\mathscr{S}}_1$. One can easily see that $\widetilde{\mathscr{R}}_1(\Phi_j)$ is isomorphic to the space $\widetilde{\mathscr{R}}_1$ defined in (2.84), which shows that the restriction to a face of the space of approximation is isomorphic to a subspace of the 2D $H(curl, \Omega)$ space.

The corresponding quadrature formula is

$$\int_T f(\underline{x})\, \mathrm{d}\underline{x} \simeq \frac{\mathrm{mes}(\hat{T}_3)}{6} \sum_{(\ell,m)\in\mathscr{I}} f(M_{\ell m}), \tag{2.77}$$

where $\mathscr{I} = \{(p, q) \in \{1, 2, 3, 4\}^2 \text{ such that } p < q\}$.

2.5.4.2 The Second-Order Element

Paradoxically, the second-order element is easier to define than the first-order one. Its degrees of freedom are the three components of a function in the basis composed of the three unit vectors at each vertex and, on the other hand, its three components on an orthonormal basis at the center G_j of a face Φ_j, composed of the unit outward normal at this point and two arbitrary orthogonal unit vectors parallel to the face (Fig. 2.12). The space of polynomials for which this set of degrees of freedom is unisolvent can be constructed as follows:

Let $\mathscr{V}_2$ be the eight-dimensional space generated by the vectors

$$\begin{pmatrix} \hat{x}_2^2 \\ -\hat{x}_1\hat{x}_2 \\ 0 \end{pmatrix}, \begin{pmatrix} 0 \\ -\hat{x}_2\hat{x}_3 \\ \hat{x}_2^2 \end{pmatrix}, \begin{pmatrix} -\hat{x}_1\hat{x}_2 \\ \hat{x}_1^2 \\ 0 \end{pmatrix}, \begin{pmatrix} -\hat{x}_2\hat{x}_3 \\ 0 \\ \hat{x}_1^2 \end{pmatrix},$$

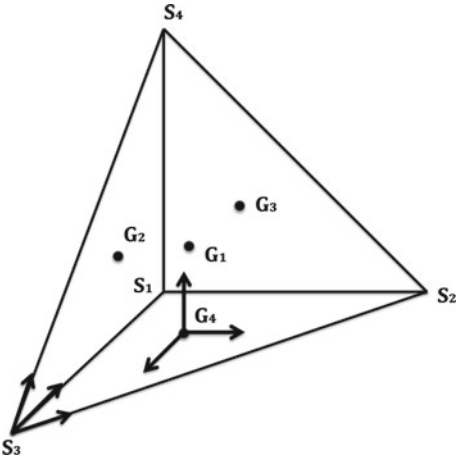

Fig. 2.12 The locations of the degrees of freedom and the three degrees of freedom at the point G_4 for $\widetilde{\mathscr{P}}_2$

$$\begin{pmatrix} \hat{x}_3^2 \\ 0 \\ -\hat{x}_1\hat{x}_3 \end{pmatrix}, \begin{pmatrix} 0 \\ \hat{x}_3^2 \\ -\hat{x}_2\hat{x}_3 \end{pmatrix}, \begin{pmatrix} \hat{x}_2\hat{x}_3 \\ -\hat{x}_1\hat{x}_3 \\ 0 \end{pmatrix}, \begin{pmatrix} 0 \\ \hat{x}_1\hat{x}_3 \\ -\hat{x}_1\hat{x}_2 \end{pmatrix}$$

and

$$\mathscr{S}_2 = [P_3(T)]^3 \oplus \mathscr{V}_2. \tag{2.78}$$

The polynomial space $\widetilde{\mathscr{P}}_2$ of dimension 24 (instead of 20 for the first family and 30 for the second family of second-order Nédélec's elements), for which the set of degrees of freedom is unisolvent, is

$$\widetilde{\mathscr{P}}_2 = \mathscr{S}_2 \oplus \{\underline{w}_1, \underline{w}_2, \underline{w}_3, \underline{w}_4\}, \tag{2.79}$$

where

$$\underline{w}_p = \lambda_\ell \lambda_m \lambda_n \nabla \lambda_p$$

and $\{\ell, m, n, p\}$ is a circular permutation of $\{1, 2, 3, 4\}$.

The corresponding quadrature formula is

$$\int_T f(\underline{x})\, \mathrm{d}\underline{x} \simeq \mathrm{mes}(\hat{T}_3) \left[\frac{3}{80} \sum_{p=1}^{4} f(G_p) + \frac{1}{720} \sum_{q=1}^{4} f(S_q) \right]. \tag{2.80}$$

One could a priori expect to obtain two points per edge with three degrees of freedom at each point. The quadrature formula was actually sought for this arrangement of points but the unique computed result was that the two points on the edges

were moved to its ends. The dimension of $\widetilde{\mathscr{S}}_2$ shows that this element (also called a *vertex element*) seems to be between the first and the second families of Nédélec's elements. A similar element can be constructed in 2D.

The stability conditions for a regular mesh in a homogeneous isotropic medium such that $c = \sqrt{\varepsilon\mu}$ are, for a leapfrog scheme on a regular mesh composed of cubic cells divided into six tetrahedra (which provides 43 classes of degrees of freedom for $\widetilde{\mathscr{S}}_1$ and 62 for $\widetilde{\mathscr{S}}_2$!) [46]:

- $c\Delta t/h \leq 0.18$ for the first-order element,
- $c\Delta t/h \leq 0.21$ for the second-order element.

Remarks:

1. As for classical edge elements, one can deduce basis functions on an element of any shape by using (2.64).
2. This element has a surprisingly large stability condition and low number of degrees of freedom.
3. The third-order element contains too many degrees of freedom to be efficient.

2.5.5 Triangular Mass-Lumped Edge Elements

For a triangle, it is possible to define the basis functions on a triangle T of any shape. Therefore, we assume that the two basis functions at a point (which is not a vertex) are tangential and normal to the edges. At a vertex, they are tangential to the two edges. The degrees of freedom are defined in the same way.

2.5.5.1 The First-Order Element

The lower-order triangular edge element with mass-lumping is derived from the lower-order edge element given in [40]. Its six degrees of freedom are the values of the tangential and normal components at the midpoint of each edge of the triangle (Fig. 2.13). The number of its degrees of freedom would naturally suggest taking its basis functions in $(P_1)^2$. However, this set of degrees of freedom is not $(P_1)^2$-unisolvent. In order to construct the good space of approximation, we introduce the barycentric coordinates $(\lambda_1, \lambda_2, \lambda_3)$ of a point M of T such that, for any point O of $\mathbb{R}^2$, we have

$$\underline{OM} = \lambda_1 \underline{OS_1} + \lambda_2 \underline{OS_2} + \lambda_3 \underline{OS_3}, \tag{2.81}$$

where (S_1, S_2, S_3) are the vertices of T.

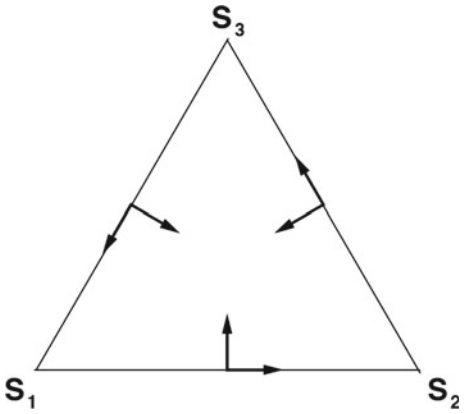

Fig. 2.13 The first-order triangular edge element with mass-lumping

We also introduce the set of functions

$$\mathscr{R}_1 = \{\underline{u} = \underline{a} + b(x_2, -x_1)^T,\ \underline{a} \in \mathbb{R}^2, b \in \mathbb{R}\} \tag{2.82}$$

and the three basis functions

$$\underline{w}_1 = \nabla\lambda_1\lambda_2\lambda_3, \tag{2.83a}$$

$$\underline{w}_2 = \lambda_1\nabla\lambda_2\lambda_3, \tag{2.83b}$$

$$\underline{w}_3 = \lambda_1\lambda_2\nabla\lambda_3. \tag{2.83c}$$

So, we can define

$$\widetilde{\mathscr{R}}_1 = \mathscr{R}_1 \oplus \{\underline{w}_1, \underline{w}_2, \underline{w}_3\}, \tag{2.84}$$

for which the set of degrees of freedom is unisolvent.

Of course, we have here two kinds of basis functions:

- 3 basis functions corresponding to the normal components:

$$\underline{w}_j^{\nu} = \frac{4}{||\nabla\lambda_j||}\underline{w}_j,\ \ j = 1\ldots 3, \tag{2.85}$$

- 3 basis functions corresponding to the tangential components (which are actually the basis functions of $\mathscr{R}_1$):

$$\underline{w}_j^{\tau} = \underline{u}_j + \sum_{\ell=1}^{3}\alpha_{j\ell}\underline{w}_{\ell}^{\nu}, \tag{2.86}$$

where $\underline{u}_j = \nabla\lambda_m\lambda_n - \nabla\lambda_n\lambda_m$, $(m,n) \in \{1,2,3\}^2$, $m \neq j$, $n \neq j$, $\alpha_{j\ell} = -(\underline{u}_j \cdot \underline{\nu})(M_\ell)$. $\underline{\nu}$ is the unit outward normal to ∂T and M_ℓ is the midpoint of the edge opposite to the vertex S_ℓ.

The appropriate quadrature formula is, of course, given by

$$\int_T f(\underline{x})\,\mathrm{d}\underline{x} \simeq \frac{\mathrm{mes}(T)}{3}\sum_{\ell=1}^{3} f(M_\ell), \tag{2.87}$$

where $\mathrm{mes}(T)$ is the measure of the triangle.

2.5.5.2 The Second-Order Element

In order to define the second-order element, we first introduce some additional notations. For each edge of T, we denote by M_{pq} the point of the edge S_pS_q such that

$$\underline{S_pM_{pq}} = \alpha\underline{S_pS_q}, \tag{2.88}$$

where α is a given real constant. At each point M_{pq}, we define two degrees of freedom which are the values of the normal and tangential components of a function and at G, the two components of the functions in the two directions of space are the degrees of freedom (Fig. 2.14).

Let $\mathscr{V}_2$ be the space of polynomials generated by the vectors $(x_2^2, -x_1x_2)^T$, $(-x_1x_2, x_1^2)^T$,

$$\mathscr{R}_2 = (P_1(T))^2 \oplus \mathscr{V}_2, \tag{2.89}$$

and

$$\underline{w}_{mn} = \nabla\lambda_\ell\lambda_m\lambda_n\phi_{nm}, \tag{2.90a}$$

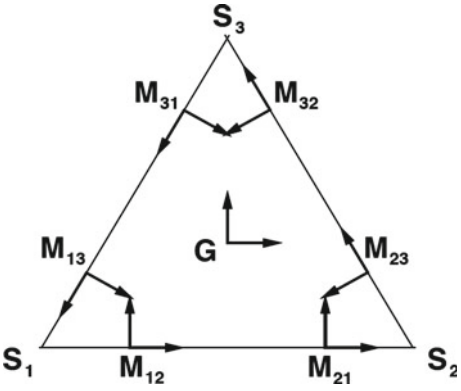

Fig. 2.14 The second-order triangular edge element with mass-lumping

$$\underline{w}_{nm} = \nabla\lambda_\ell\lambda_m\lambda_n\phi_{mn}, \tag{2.90b}$$

where $(\ell, m, n) \in \{1, 2, 3\}^3$ and are all different, and ϕ_{nm} is the polynomial of P_1 defined by $\phi_{nm}(G) = \phi_{nm}(M_{nm}) = 0$ and $\phi_{nm}(M_{mn}) = 1$.

With the above notations, we can define the space of polynomials $\widetilde{\mathscr{R}}_2$ for which the set of degrees of freedom is unisolvent

$$\widetilde{\mathscr{R}}_2 = \mathscr{R}_2 \oplus \{\underline{w}_{12}, \underline{w}_{21}, \underline{w}_{13}, \underline{w}_{31}, \underline{w}_{23}, \underline{w}_{32}\}. \tag{2.91}$$

The corresponding quadrature rule to obtain mass-lumping is given by

$$\int_T f(\underline{x})\,\mathrm{d}\underline{x} \simeq \mathrm{mes}(T)\left[\frac{9}{40}f(G) + \frac{11}{240}\sum_{(p,q)} f(M_{pq})\right], \tag{2.92}$$

where $(p, q) \in \{1, 2, 3\}^2$ and $p \neq q$.

Stability conditions for a regular mesh in a homogeneous isotropic medium such that $c = \sqrt{\varepsilon\mu}$ are, for a leapfrog scheme on a regular mesh composed of rectangle triangles [46]:

- $c\Delta t/h \leq 0.2654$ for the first-order element,
- $c\Delta t/h \leq 0.1167$ for the second-order element.

Remark: A third-order element was studied in [46] but was less efficient than the second-order one because of its large number of degrees of freedom. For this reason, we do not describe it here.

2.6 Hexahedral and Quadrilateral Edge Elements

Both families of Nédélec's edge elements can be defined on hexahedra and quadrilaterals. However, the polynomial spaces involved in these elements are much easier to define. They actually are tensor products of 1D polynomial spaces.

2.6.1 First Family

2.6.1.1 Modal Definition

This family will be first defined in a modal way [40] on the unit cube $\widehat{K} = [0, 1]^3$. The polynomial space corresponding to this family reads

$$\mathscr{Q}_r = \left\{\underline{u} \text{ such that } u_1 \in Q_{r-1,r,r},\ u_2 \in Q_{r,r-1,r},\ u_3 \in Q_{r,r,r-1}\right\}, \tag{2.93}$$

where

$$Q_{pqr}(\hat{\underline{x}}) = P_p(\hat{x}_1) \times P_q(\hat{x}_2) \times P_r(\hat{x}_3)$$
$$= \left\{ v(\hat{\underline{x}}) = \sum_{i=0}^{p} \sum_{j=0}^{q} \sum_{k=0}^{r} a_{i,j,k}\, \hat{x}_1^i \hat{x}_2^j \hat{x}_3^k, \quad a_{i,j,k} \in \mathbb{R} \right\}. \tag{2.94}$$

Obviously,

$$\dim \mathscr{Q}_r = 3r(r+1)^2. \tag{2.95}$$

The modal degrees of freedom related to this family are

1. $12r$ integrals on the edges defined by

$$\int_e \underline{u} \cdot \underline{t} q \, \mathrm{d}\hat{\sigma}, \quad \forall q \in P_{r-1},$$

where $\underline{t}$ is the unit vector along an edge $e \in \widehat{K}$.

2. $6 \times 2r(r-1)$ integrals on the faces defined by

$$\int_f (\underline{u} \times \underline{n}) \cdot \underline{q} \, \mathrm{d}\hat{\underline{\gamma}}, \quad \forall \underline{q} = (q_1, q_2) \text{ such that } q_1 \in Q_{r-2,r-1},\ q_2 \in Q_{r-1,r-2},$$

where $\underline{n}$ is the unit vector normal to a face $f \in \widehat{K}$.

3. $3r(r-1)^2$ integrals in $\widehat{K}$ defined by

$$\int_{\widehat{K}} \underline{u} \cdot \underline{q} \, \mathrm{d}\hat{\underline{x}}, \quad \forall \underline{q} = (q_1, q_2, q_3)$$
$$\text{such that } q_1 \in Q_{r-1,r-2,r-2},\ q_2 \in Q_{r-2,r-1,r-2},\ q_3 \in Q_{r-2,r-2,r-1}.$$

Of course, $12r + 6 \times 2r(r-1) + 3r(r-1)^2 = 3r(r+1)^2$.

Extension to any hexahedron K_i is made by the $H(curl)$-conform transform defined in (2.64) in which DF_T is replaced by DF_i, where DF_i is the Jacobian matrix of the mapping $\underline{F}_i$ defined in (2.24).[9] This extension holds for any hexahedral or quadrilateral edge element.

2.6.1.2 Nodal Definition

The tensor character of $\mathscr{Q}_r$ enables us to define the degrees of freedom in a nodal way by using vector values of the basis functions in the three canonical directions.

[9] The (not obvious) $H(curl)$-conform character of this mapping for hexahedra is proven in the Annex of [8].

However, in order to agree with the definition of the spaces, we must use different sets of points for each direction. Actually, we need $r \times (r+1) \times (r+1)$ points in the $\hat{x}_1$ direction, $(r+1) \times r \times (r+1)$ in the $\hat{x}_2$ direction and $(r+1) \times (r+1) \times r$ in the $\hat{x}_3$ direction. This structure allows us to choose r Gauss points and $r+1$ Gauss-Lobatto points for the coordinates [47] (Fig. 2.15).

Let $\left(\hat{\xi}_\ell^G\right)_{\ell=1}^{r}$ and $\left(\hat{\xi}_\ell^{GL}\right)_{\ell=1}^{r+1}$ be respectively the sets of $(r-1)$-order Gauss and r-order Gauss-Lobatto points. We can define the $(n-1)$th-order 1D Lagrange polynomials

$$\varphi_j^A(x) = \frac{\prod_{\ell=1,\ell\neq j}^{n} \left(x - \hat{\xi}_\ell^A\right)}{\prod_{\ell=1,\ell\neq j}^{n} \left(\hat{\xi}_j^A - \hat{\xi}_\ell^A\right)}, \quad j = 1 \ldots n, \tag{2.96}$$

where $A = G$ and $n = r$ for Gauss points and $A = GL$ and $n = r+1$ for Gauss-Lobatto points.

With these notations, the basis functions read

$$\hat{\varphi}_{i,j,k}(\hat{x}_1, \hat{x}_2, \hat{x}_3)\, \underline{e}_1 = \hat{\varphi}_i^G(\hat{x}_1)\, \hat{\varphi}_j^{GL}(\hat{x}_2)\, \hat{\varphi}_k^{GL}(\hat{x}_3)\, \underline{e}_1, \tag{2.97a}$$

$$\hat{\varphi}_{i,j,k}(\hat{x}_1, \hat{x}_2, \hat{x}_3)\, \underline{e}_2 = \hat{\varphi}_i^{GL}(\hat{x}_1)\, \hat{\varphi}_j^{G}(\hat{x}_2)\, \hat{\varphi}_k^{GL}(\hat{x}_3)\, \underline{e}_2, \tag{2.97b}$$

$$\hat{\varphi}_{i,j,k}(\hat{x}_1, \hat{x}_2, \hat{x}_3)\, \underline{e}_3 = \hat{\varphi}_i^{GL}(\hat{x}_1)\, \hat{\varphi}_j^{GL}(\hat{x}_2)\, \hat{\varphi}_k^{G}(\hat{x}_3)\, \underline{e}_3. \tag{2.97c}$$

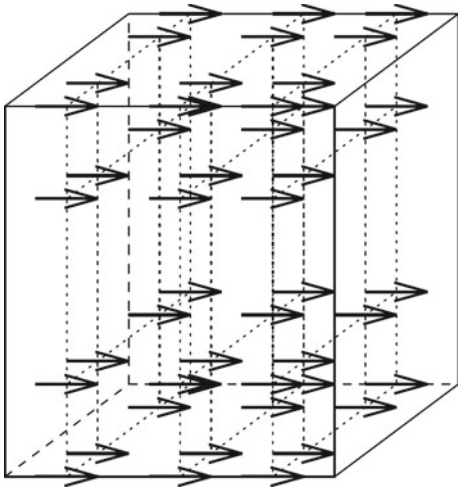

Fig. 2.15 The locations of the degrees of freedom of the first family of edge elements for $r = 3$ in the $\hat{x}_2$ direction on the unit cube

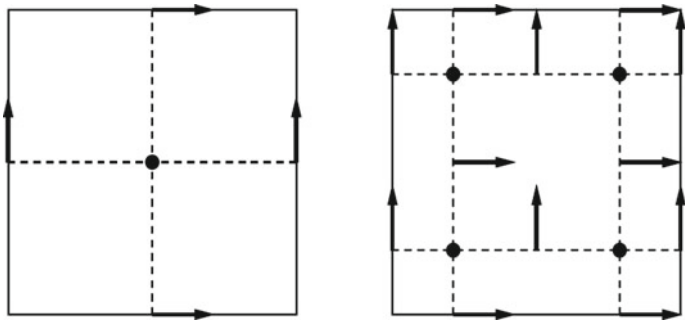

Fig. 2.16 The locations of the degrees of freedom of the first family of edge elements on the unit square for $r = 1$ (*left*) and $r = 2$ (*right*) in both directions. The *dashed lines* indicate the Gauss points

2.6.1.3 Quadrilateral Elements

A modal definition of quadrilateral edge elements is useless. So, we define them in a nodal way, which is very similar to hexahedra. The polynomial space on the unit square $\widehat{K} = [0, 1]^2$ is

$$\mathscr{Q}_r = \left\{ \underline{u} \text{ such that } u_1 \in Q_{r-1,r},\ u_2 \in Q_{r,r-1} \right\}. \tag{2.98}$$

As for the cube, we have $r \times (r + 1)$ points in the $\hat{x}_1$ direction, $(r + 1) \times r$ in the $\hat{x}_2$ direction, which enables us to mix Gauss and Gauss-Lobatto points (Fig. 2.16).

Basis functions obviously read

$$\hat{\varphi}_{i,j}(\hat{x}_1, \hat{x}_2)\, \underline{e}_1 = \hat{\varphi}_i^G(\hat{x}_1)\, \hat{\varphi}_j^{GL}(\hat{x}_2)\, \underline{e}_1, \tag{2.99a}$$

$$\hat{\varphi}_{i,j}(\hat{x}_1, \hat{x}_2)\, \underline{e}_2 = \hat{\varphi}_i^{GL}(\hat{x}_1)\, \hat{\varphi}_j^G(\hat{x}_2)\, \underline{e}_2. \tag{2.99b}$$

As we shall see later, this choice leads to mass-lumping on an orthogonal mesh, but not on elements of any shape (even with parallel faces). It provides a variational generalization of the Yee scheme [8, 48].

2.6.2 Second Family

2.6.2.1 Modal Definition

The polynomial space associated to the second family of hexahedra on the unit cube is simply $(Q_r)^3$, where Q_r is defined as in (2.17) with $d = 3$.

The degrees of freedom of this family are defined in [41] in a modal way as follows

1. $12(r+1)$ integrals on the edges defined by

$$\int_e \underline{u} \cdot \underline{t} q \, \mathrm{d}\hat{\sigma}, \quad \forall q \in P_r,$$

where $\underline{t}$ is the unit vector along an edge $e \in \widehat{K}$.

2. $6 \times 2r(r^2-1)$ integrals on the faces defined by

$$\int_f \underline{u} \cdot \underline{q} \, \mathrm{d}\hat{\underline{\gamma}}, \quad \forall \underline{q} = (q_1, q_2) \text{ such that } q_1 \in Q_{r,r-2},\ q_2 \in Q_{r-2,r},$$

where f is a face of $\widehat{K}$.

3. $3(r^2-1)(r-1)$ integrals in $\widehat{K}$ defined by

$$\int_{\widehat{K}} \underline{u} \cdot \underline{q} \, \mathrm{d}\underline{\hat{x}}, \quad \forall \underline{q} = (q_1, q_2, q_3)$$

$$\text{such that } q_1 \in Q_{r,r-2,r-2},\ q_2 \in Q_{r-2,r,r-2},\ q_3 \in Q_{r-2,r-2,r}.$$

Obviously, $12(r+1)+6\times 2r(r^2-1)+3(r^2-1)(r-1) = 3(r+1)^3 = \dim (Q_r)^3$.

2.6.2.2 Nodal Definition

The nodal definition of the degrees of freedom is quite trivial. Following the polynomial space definition, it is sufficient to define the vector-valued basis functions by their values at $(r+1)^3$ Gauss-Lobatto points. So, the basis functions $\hat{\varphi}_{i,j,k}\, \underline{e}_p$, $\underline{e}_p$ being a vector of the canonical basis of $\mathbb{R}^3$, $p = 1 \ldots 3$ read

$$\hat{\varphi}_{i,j,k}(\hat{x}_1, \hat{x}_2, \hat{x}_3)\, \underline{e}_p = \hat{\varphi}_i^{GL}(\hat{x}_1)\, \hat{\varphi}_j^{GL}(\hat{x}_2)\, \hat{\varphi}_k^{GL}(\hat{x}_3)\, \underline{e}_p, \quad p = 1 \ldots 3. \tag{2.100}$$

Although trivial, by using the $H(curl)$-conform transform, this definition keeps the tangential continuity over the mesh since the tangents to the edges and the faces of the cube are actually in the directions of the vectors of the canonical basis of $\mathbb{R}^3$.

2.6.2.3 Quadrilateral Elements

The nodal definition of quadrilateral elements is quite obvious for this family. The polynomial space on unit square is $(Q_r)^2$ and the vector-valued basis functions (defined by their values at $(r+1)^2$ Gauss-Lobatto points) read (Fig. 2.17).

$$\hat{\varphi}_{i,j,k}(\hat{x}_1, \hat{x}_2)\, \underline{e}_p = \hat{\varphi}_i^{GL}(\hat{x}_1)\, \hat{\varphi}_j^{GL}(\hat{x}_2)\, \underline{e}_p, \quad p = 1, 2.$$

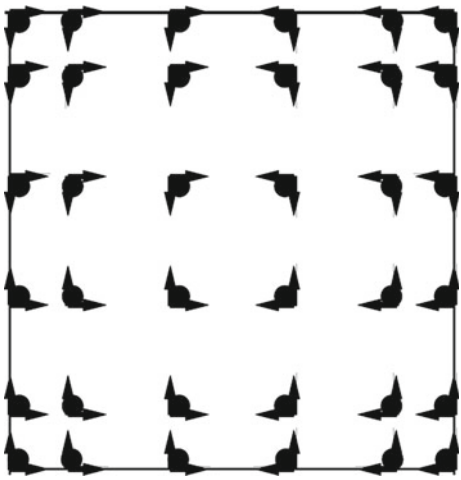

Fig. 2.17 The locations of the degrees of freedom on the unit square for $r = 5$ in both directions. The *black* points indicate the Gauss-Lobatto points

As we shall see, the nodal definition of the second family enables mass-lumping on any type of hexahedral or quadrilateral mesh [49] but does not provide spurious free approximations [14, 50].

2.7 $H(div)$ Finite Elements

$H(div)$ finite elements were constructed in order to keep the normal continuity of vector-valued functions. Their presence in this book is justified because they are the natural complementary elements to edge elements for Maxwell's equations [42, 51]. So, we just give in this section the guidelines to construct these elements.

2.7.1 Tetrahedral and Triangular Elements

2.7.1.1 First Family

The polynomial space associated to $\hat{T}_3$ is

$$D_r = (P_{r-1})^3 \oplus \underline{\hat{x}}\,\widetilde{P}_r \tag{2.101}$$

with $\widetilde{P}_r$ defined as in (2.58).

Obviously, $\dim D_r = \dfrac{1}{2} r(r+1)(r+3)$.

Following [40], we have two types of degrees of freedom:

1. $2r(r+1)$ integrals on the faces defined by

$$\int_f \underline{u} \cdot \underline{n}\, q \, \mathrm{d}\underline{\hat{\gamma}}, \quad \forall q \in P_{r-1},$$

where f is a face of $\widehat{K}$ and $\underline{n}$ the exterior unit normal to f.

2. $r(r^2-1)/2$ integrals in $\hat{T}_3$ defined by

$$\int_{\hat{T}_3} \underline{u} \cdot \underline{q} \, \mathrm{d}\underline{\hat{x}}, \quad \forall \underline{q} \in (P_{r-2})^3.$$

One can easily check that $2r(r+1) + r(r^2-1)/2 = r(r+1)(r+3)/2$.

Now, in order to keep the normal continuity of a function $\underline{\varphi}$ over a mesh, one must deduce $\underline{\varphi}$ on any tetrahedron T of the mesh from a function $\underline{\hat{\varphi}}$ on the unit element $\hat{T}_3$ by using the $H(div)$-conform transform (also called Piola's transform) which reads

$$\underline{\varphi} \circ \underline{F}_T = \frac{1}{J_T} DF_T \, \underline{\hat{\varphi}}, \tag{2.102}$$

where $J_T = \det DF_T$, $\underline{F}_T$ and DF_T being defined as in Sect. 2.5.2.

Here also, this element can be defined in a nodal way by using $2r(r+1)$ pointwise values of vector-valued functions orthogonal the faces and $r(r^2-1)/2$ values of vector-valued interior functions collinear to the canonical basis of $\mathbb{R}^3$.

The polynomial space corresponding to the unit triangular element $\hat{T}_2$ is the space $\mathscr{R}_r^T$ defined in (2.65). The degrees of freedom are

1. $3r$ integrals on the edges defined by

$$\int_e \underline{u} \cdot \underline{n}\, q \, \mathrm{d}\hat{\sigma}, \quad \forall q \in P_{r-1},$$

where is the exterior unit vector normal to an edge $e \in \hat{T}_2$.

2. $r(r-1)$ integrals in $\hat{T}_2$ defined by

$$\int_{\hat{T}_2} \underline{u} \cdot \underline{q} \, \mathrm{d}\underline{\hat{x}}, \quad \forall \underline{q} \in (P_{r-2})^2,$$

or in a nodal way, by using pointwise values of r vector-valued functions normal to each edge and $r(r-1)$ interior vector-valued functions collinear to the canonical basis of $\mathbb{R}^2$.

Extension to any triangle T is made by using (2.102).

2.7.1.2 Second Family

A modal definition of the second family would be tedious and useless in practice. Since the polynomial space for this family is $(P_r)^3$ on $\hat{T}_3$ ($(P_r)^2$ on $\hat{T}_2$), the degrees of freedom can be defined by pointwise values of three (two in 2D) vector-valued function at each Hesthaven's point as follows:

- In 3D
  1. Three functions normal to the faces at a summit,
  2. One function normal to the face and two functions tangent to the face (and orthogonal to each other) at a point on a face,
  3. Three functions collinear to the canonical basis of $\mathbb{R}^3$ at an interior point.
- In 2D
  1. Two functions normal to the edges at a summit,
  2. Two functions collinear to the canonical basis of $\mathbb{R}^2$ at an interior point.

Extension to any element T is made by using (2.102).

2.7.2 *Hexahedral and Quadrilateral Elements*

2.7.2.1 First Family

Hexahedral and quadrilateral elements are constructed in a way very similar to edge elements. For hexahedra, the polynomial space is

$$\mathscr{Q}'_r = \left\{ \underline{u} \text{ s.t. } u_1 \in Q_{r,r-1,r-1},\ u_2 \in Q_{r-1,r,r-1},\ u_3 \in Q_{r-1,r-1,r} \right\}, \tag{2.103}$$

With the notations used in (2.96), the basis functions read

$$\hat{\varphi}_{i,j,k}(\hat{x}_1, \hat{x}_2, \hat{x}_3)\, \underline{e}_1 = \hat{\varphi}_i^{GL}(\hat{x}_1)\, \hat{\varphi}_j^{G}(\hat{x}_2)\, \hat{\varphi}_k^{G}(\hat{x}_3)\, \underline{e}_1, \tag{2.104a}$$

$$\hat{\varphi}_{i,j,k}(\hat{x}_1, \hat{x}_2, \hat{x}_3)\, \underline{e}_2 = \hat{\varphi}_i^{G}(\hat{x}_1)\, \hat{\varphi}_j^{GL}(\hat{x}_2)\, \hat{\varphi}_k^{G}(\hat{x}_3)\, \underline{e}_2, \tag{2.104b}$$

$$\hat{\varphi}_{i,j,k}(\hat{x}_1, \hat{x}_2, \hat{x}_3)\, \underline{e}_3 = \hat{\varphi}_i^{G}(\hat{x}_1)\, \hat{\varphi}_j^{G}(\hat{x}_2)\, \hat{\varphi}_k^{GL}(\hat{x}_3)\, \underline{e}_3. \tag{2.104c}$$

The degrees of freedom are defined in the same way as edge elements (Fig. 2.18). For quadrilaterals, the polynomial space is

$$\mathscr{Q}'_r = \left\{ \underline{u} \text{ such that } u_1 \in Q_{r,r-1},\ u_2 \in Q_{r-1,r} \right\}, \tag{2.105}$$

and basis functions read

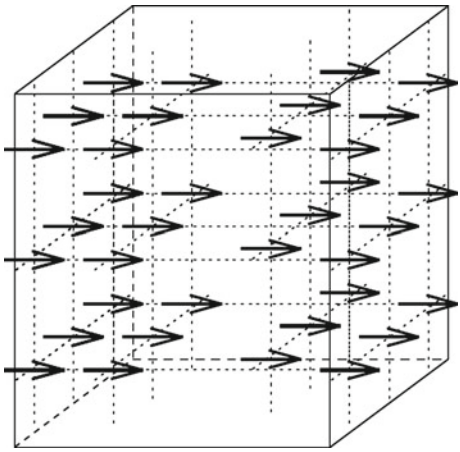

Fig. 2.18 The locations of the degrees of freedom of the first family of $H(div)$ elements for $r = 3$ in the $\hat{x}_2$ direction on the unit cube

$$\hat{\varphi}_{i,j,k}(\hat{x}_1, \hat{x}_2)\, \underline{e}_1 = \hat{\varphi}_i^{GL}(\hat{x}_1)\, \hat{\varphi}_j^{G}(\hat{x}_2)\, \underline{e}_1, \tag{2.106a}$$

$$\hat{\varphi}_{i,j,k}(\hat{x}_1, \hat{x}_2)\, \underline{e}_2 = \hat{\varphi}_i^{G}(\hat{x}_1)\, \hat{\varphi}_j^{GL}(\hat{x}_2)\, \underline{e}_2. \tag{2.106b}$$

The degrees of freedom are obvious (Fig. 2.19).

Extension to elements of any shape K_i in 2D or 3D is made by using the $H(div)$-conform transform

$$\underline{\varphi} \circ \underline{F}_i = \frac{1}{J_i} DF_i\, \underline{\hat{\varphi}}, \tag{2.107}$$

with $J_i = \det DF_i$ and $\underline{F}_i$ defined in (2.23) and (2.24).

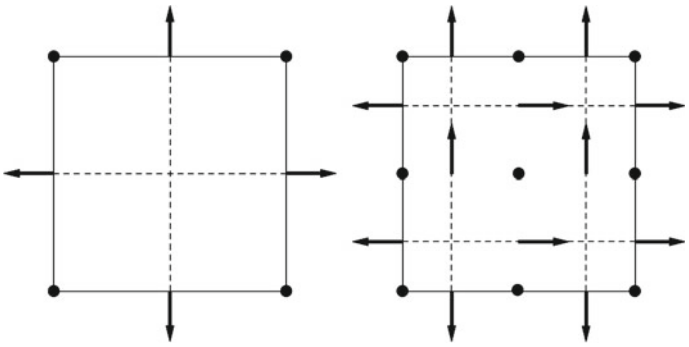

Fig. 2.19 The locations of the degrees of freedom of the first family of $H(div)$ elements on the unit square for $r = 1$ (*left*) and $r = 2$ (*right*) in both directions. The *dashed lines* indicate the Gauss points

2.7.2.2 Second Family

The second family of $H(div)$ elements is defined on the unit cube or square exactly as edge elements. The only difference lies in the the extension to elements of any shape which is made by using (2.107). This definition is justified by the both tangent and normal character of each nodal degree of freedom at any point for the second family.

Remark: Unlike 3D elements, 2D first families of edge and $H(div)$ elements have exactly the same number of degrees of freedom. This comes from the fact that 3D edge elements have degrees of freedom located on edges, faces and inside the elements whereas the degrees of freedom of $H(div)$ elements are only on the faces and inside the element. However, in 2D both types of element have their degrees of freedom on edges and inside. In 2D, we can say that $H(div)$ degrees of freedom are somehow orthogonal to these of edge elements (cf. Figs. 2.16 and 2.19).

2.8 Other Mixed Elements

In this section, we provide the guidelines to construct edge and $H(div)$ elements on pyramids and wedges, which can be useful for solving Maxwell's equations in frequency domain. A wider description of such elements can be found in [52, 53]

2.8.1 Pyramidal and Prismatic Edge Elements

2.8.1.1 Pyramids

The approximate space of edge elements on the unit pyramid corresponding to the first family of Nédélec's elements reads

$$\begin{aligned}\mathscr{P}_r^e = (\mathscr{P}_{r-1})^3 \oplus \left\{ \frac{\hat{x}_1^p \hat{x}_2^p}{(1-\hat{x}_3)^{p+2}} \underline{w}_1,\ 0 \le p \le r-1 \right\} \\ \oplus \left\{ \frac{\hat{x}_1^m \hat{x}_2^{n+2}}{(1-\hat{x}_3)^{m+2}} \underline{w}_2, \frac{\hat{x}_1^{n+2} \hat{x}_2^m}{(1-\hat{x}_3)^{m+2}} \underline{w}_3,\ 0 \le m \le n \le r-2 \right\} \\ \oplus \left\{ \frac{\hat{x}_1^p \hat{x}_2^q}{(1-\hat{x}_3)^{p+q-r+1}} \underline{w}_1, \frac{\hat{x}_1^q \hat{x}_2^p}{(1-\hat{x}_3)^{p+q-r+1}} \underline{w}_2, \begin{array}{l} 0 \le p \le r-1, \\ 0 \le q \le r \end{array} \right\},\end{aligned} \tag{2.108}$$

where

$$\underline{w}_1 = \begin{pmatrix} \hat{x}_2(1-\hat{x}_3) \\ \hat{x}_1(1-\hat{x}_3) \\ \hat{x}_1\hat{x}_2 \end{pmatrix}, \ \underline{w}_2 = \begin{pmatrix} 1-\hat{x}_3 \\ 0 \\ \hat{x}_1 \end{pmatrix}, \ \underline{w}_3 = \begin{pmatrix} 0 \\ 1-\hat{x}_3 \\ \hat{x}_2 \end{pmatrix}$$

and $\mathscr{P}_r$ defined in (2.46). We have

$$\dim \mathscr{P}_r^e = \frac{r(2r^2+9r+5)}{2}.$$

The degrees of freedom on the faces of this element coincide with these of the first family tetrahedral and hexahedral edge elements. So, $\dim \mathscr{P}_r^e$ can be decomposed into

- r degrees of freedom on each edge ($8r$ for all the edges),
- $2r(r-1)$ degrees of freedom on the quadrilateral face,
- $r(r-1)$ degrees of freedom on a triangular face ($4r(r-1)$ for the four faces),
- $r(r-1)(2r-1)/2$ interior degrees of freedom.

As for other elements, a second family can be constructed by using $(\mathscr{P}_r)^3$.

For both families, a function $\underline{\varphi}$ on a pyramid of any shape can be deduced from a function $\hat{\underline{\varphi}} \in \mathscr{P}_r^e$ as follows

$$\underline{\varphi} \circ \underline{F}^{\pi} = (DF^{\pi})^{*-1}\hat{\underline{\varphi}}, \tag{2.109}$$

where $\underline{F}^{\pi}$ is defined by (2.47).

2.8.1.2 Wedges

The polynomial space for edge elements on the unit prism $\hat{W}$ reads

$$\mathscr{P}_{e,r}^w = (\mathscr{R}_r^T(\hat{x}_1,\hat{x}_2) \otimes P_r(\hat{x}_3)) \times (P_r(\hat{x}_1,\hat{x}_2) \otimes P_{r-1}(\hat{x}_3)), \tag{2.110}$$

where $\mathscr{R}_r^T$ defined as in (2.65).

A simple computation shows that

$$\dim \mathscr{P}_{e,r}^w = 3r(r+1)(r+2)/2.$$

Since the degrees of freedom on the faces must fit with those of tetrahedra and hexahedra, they are defined in exactly the same way as on pyramids, the number of interior degrees of freedom being $r(r-1)(3r-4)/2$. As for pyramids also, the second family can be deduced from Sect. 2.4.1. The mapping to a wedge of any shape is given by

$$\underline{\varphi} \circ \underline{F}^{w} = (DF^{w})^{*-1}\hat{\underline{\varphi}}, \tag{2.111}$$

where $\underline{F}^{w}$ is defined by (2.45).

2.8.2 Pyramidal and Prismatic $H(div)$ Elements

2.8.2.1 Pyramids

In this part, we give the minimal spaces which ensure the optimal convergence in $O(h^r)$ for $H(div)$ estimates (see [53] for more details about the construction). The approximate space on the unit pyramid corresponding to the first family of $H(div)$ elements reads

$$\begin{aligned}
\mathscr{P}_r^{div} &= (\mathscr{P}_{r-1})^3 \\
&\oplus \left\{ \frac{\hat{x}_1^{n+1}\hat{x}_2^m}{(1-\hat{x}_3)^{m+1}}\,\underline{e}_1 \oplus \frac{\hat{x}_1^m\hat{x}_2^{n+1}}{(1-\hat{x}_3)^{m+1}}\,\underline{e}_2,\ 0 \le m \le n \le r-1 \right\} \\
&\oplus \left\{ \frac{\hat{x}_1^m\hat{x}_2^{n+1}}{(1-\hat{x}_3)^{m+1}}\,\underline{u}_1 \oplus \frac{\hat{x}_1^{n+1}\hat{x}_2^m}{(1-\hat{x}_3)^{m+1}}\,\underline{u}_2,\ 0 \le m \le n \le r-1 \right\} \\
&\oplus \left\{ \frac{\hat{x}_1^p\hat{x}_2^q}{(1-\hat{x}_3)^{p+q-r}}\,\underline{u}_3,\ 0 \le p,q \le r \right\},
\end{aligned} \tag{2.112}$$

where $\underline{e}_1, \underline{e}_2$ are the two first vectors of the canonical basis of $\mathbb{R}^3$,

$$\underline{u}_1 = \begin{pmatrix} \dfrac{\hat{x}_1}{1-\hat{x}_3} \\ 0 \\ -1 \end{pmatrix},\ \underline{u}_2 = \begin{pmatrix} 0 \\ \dfrac{\hat{x}_2}{1-\hat{x}_3} \\ -1 \end{pmatrix} \underline{u}_3 = \begin{pmatrix} \dfrac{\hat{x}_1}{1-\hat{x}_3} \\ \dfrac{\hat{x}_2}{1-\hat{x}_3} \\ -1 \end{pmatrix}$$

and $\mathscr{P}_r$ defined in (2.46). We have

$$\dim \mathscr{P}_r^{div} = \frac{(r+1)\,(2r^2+7r+2)}{2}.$$

As for edge elements, the degrees of freedom on the faces must fit to these of the first family tetrahedral and hexahedral $H(div)$ elements. So, $\dim \mathscr{P}_r^{div}$ is decomposed into

- r^2 degrees of freedom on the quadrilateral face,
- $r(r+1)/2$ degrees of freedom on a triangular face ($2r(r+1)$ for the four faces),
- $(2r^3+3r^2+5r+2)/2$ interior degrees of freedom.

As for edge elements, a second family can be constructed by using $(\mathscr{P}_r)^3$.

2.8.2.2 Wedges

The polynomial space for $H(div)$ elements on the unit prism $\hat{W}$ reads

$$\mathscr{P}^w_{div,r} = (\mathscr{R}^T_r(\hat{x}_1, \hat{x}_2) \otimes P_{r-1}(\hat{x}_3)) \times (P_{r-1}(\hat{x}_1, \hat{x}_2) \otimes P_r(\hat{x}_3)), \tag{2.113}$$

where $\mathscr{R}^T_r$ defined as in (2.65). Obviously, we have

$$\dim \mathscr{P}^w_{div,r} = \frac{r\,(3r^2 + 6r + 1)}{2}.$$

The degrees of freedom are the same as those of pyramids on the faces and we have $r(r-1)(3r+1)/2$ interior degrees of freedom.

Mapping to an element of any shape is made by Piola's transform defined in (2.102), in which we use $\underline{F}^\pi$ for pyramids and $\underline{F}^w$ for wedges.

The second families of edge and $H(div)$ elements can immediately be deduced from Sects. 2.4.1 and 2.4.2.

Remark: References [52, 53] introduce "optimal" families by adding some degrees of freedom.

References

1. Ciarlet, P.G.: The Finite Element Method for Elliptic Problems. North-Holland (2002)
2. Ciarlet, P.G., Lions, J.-L.: Handbook of Numerical Analysis, vol. 2. North-Holland (1991)
3. Young, L.C.: An efficient finite element method for reservoir simulation. In: Proceedings of the 53rd Annual Fall Technical Conference and Exhibition of the Society of Petroleum Engineers of AIME. Houston, Texas Oct. 1–3 (1978)
4. Hennart, J.-P., Sainz, E., Villegas, M.: On the efficient use of the finite element method in static neutron diffusion calculations. Comput. Methods Nucl. Eng. **1**, 3–87 (1979)
5. Maday, Y., Patera, A.T.: Spectral element methods for the imcompressible Navier-Stokes equations. In: Noor, A.K. (ed.) State of the Art Survey in Computational Mechanics, pp. 71–143 (1989)
6. Cohen, G., Joly, P., Tordjman, N.: Higher-order finite elements with mass lumping for the 1-D wave equation. Finite Elem. Anal. Des. **17**(3–4), 329–336 (1994)
7. Tordjman, N.: Eléments finis d'ordre élevé avec condensation de masse pour l'équation des ondes, thèse de doctorat, U. Paris IX-Dauphine (1995)
8. Cohen, G.: High Order Numerical Methods for Transient Wave Equations, Scientific Computation. Springer, Heidelberg (2001)
9. Hesthaven, J.S.: From electrostatics to almost optimal nodal sets for polynomial interpolation in a simplex. SIAM J. Numer. Anal. **35**(2), 655–676 (1998)
10. Hesthaven, J.S., Warburton, T.: Nodal discontinuous Galerkin methods. In: Texts in Applied Mathematics, vol. 54. Springer, Heidelberg (2008)
11. Seriani, G., Priolo, E.: Spectral element method for acoustic wave simulation in heterogeneous media. Finite Elem. Anal. Des. **16**(3–4), 337–348 (1994)
12. Dubiner, M.: Spectral methods on triangles and other domains. J. Sci. Comput. **6**(4), 345–390 (1991)
13. Gordon, W., Hall, C.: Transfinite element methods: blending functions interpolation over arbitrary element domains. Numer. Math. **21**, 109–129 (1973)

14. Duruflé, M.: Intégration numérique et éléments finis d'ordre élevé appliqués aux équations de Maxwell en régime harmonique, thèse de doctorat, U. de Paris-Dauphine (2006)
15. Hesthaven, J.S., Teng, C.H.: Stable spectral methods on tetrahedral elements. SIAM J. Sci. Comput. **21**(6), 2352–2380 (2000)
16. Cohen, G., Elmkies, A.: Eléments finis triangulaires P_2 avec condensation de masse pour l'équation des ondes, INRIA Report RR-2418 (1994)
17. Cohen, G., Joly, P., Roberts, J.E., Tordjman, N.: Higher order triangular finite elements with mass lumping for the wave equation. SIAM J. Numer. Anal. **38**(6), 12047–2078 (2001)
18. Chin-Joe-Kong, M.J.S., Mulder, W.A., van Veldhuizen, M.: Higher-order triangular and tetrahedral finite elements with mass lumping for solving the wave equation. J. Eng. Math. **35**, 405–426 (1999)
19. Duffy, M.G.: Quadrature over a pyramid or cube of integrands with a singularity at a vertex. SIAM J. Numer. Anal. **19**(6), 1260–1262 (1982)
20. Karniadakis, G., Sherwin, S.J.: Spectral/hp Element Methods for CFD, 2nd edn. Oxford University Press, Oxford (2005)
21. Abramowitz, M., Stegun, I.A. (eds.): Handbook of Mathematical Functions. Dover Publications, New York (1972)
22. Giraldo, F.X., Taylor, M.A.: A diagonal mass matrix triangular spectral element method based on cubature points. J. Eng. Math. **56**(3), 307–322 (2006)
23. Bedrosian, G.: Shape functions and integration formulas for three-dimensional finite element analysis. Int. J. Numer. Methods Eng. **35**, 95–108 (1992)
24. Zgainski, F.X., Coulomb, J.C., Marchal, Y., Claeyssen, F., Brunotte, X.: A new family of finite elements: the pyramidal elements. IEEE Trans. Magn. **32**(3), 1393–1396 (1996)
25. Graglia, R.D., Wilton, D.R., Peterson, A.F., Gheorma, I.-L.: Higher order interpolatory vector bases on pyramidal elements. IEEE Trans. Antennas Propag. **47**(5), 775–782 (1999)
26. Chatzi, V., Preparata, F.P.: Using Pyramids in Mixed Meshes—Point Placement and Basis Functions. Brown University, Providence (2000)
27. Solín, P., Segeth, K., Dolezel, I.: Higher-order finite elements methods. In: Studies in Advanced Mathematics. Chapman and Hall, London (2003)
28. Szabó, B.A., Babuška, I.: Finite Element Analysis. Wiley, New York (1991)
29. Sherwin, S.J.: Hierarchical HP finite element in hybrid domains. Finite Elem. Anal. Des. **27**(1), 109–119 (1997)
30. Sherwin, S.J., Warburton, T., Karniadakis, G.E.: Spectral/HP methods for elliptic problems on hybrid grids. Contemp. Math. **218**, 191–216 (1998)
31. Warburton, T.: Spectral/HP Methods on Polymorphic Multi-Domains: Algorithms and Applications. Brown University, Providence (1999)
32. Bergot, M., Cohen, G., Duruflé, M.: Higher-order finite element for hybrid meshes using new nodal pyramidal elements. J. Sci. Comput. **42**(3), 345–381 (2010)
33. Zaglmayr, S.: High order finite element methods for electromagnetic field computation, Ph.D. thesis, Johannes Kepler University, Linz Austria (2006)
34. Radau, R.: Etudes sur les formules d'approximation qui servent à calculer la valeur d'une intégrale définie. J. Math. Pures Appl. **6**, 283–336 (1880)
35. Zienkiewicz, O.C., Taylor, R.L., Zhu, J.Z.: The Finite Element Method: Its Basis and Fundamentals. Elsevier, Amsterdam (2005)
36. Bergot, M.: Eléments finis d'ordre élevé pour maillages hybrides. Application à la résolution de systèmes hyperboliques linéaires en régimes harmonique et temporel, thèse de doctorat, U. de Paris-Dauphine (Paris IX) (2010)
37. Bergot, M., Duruflé, M.: Higher-order discontinuous Galerkin method for pyramidal elements using orthogonal basis. Numer. Methods Part. Differ. Eq. **29**(1), 144–169 (2013)
38. Fraeijs de Veubeke, B.M.: Displacement and Equilibrium Models in Stress Analysis. In: Zienkiewicz, O.C., Hollister, G. (eds.) pp. 145-197. Wiley, London (1965), (reprinted in Int. J. Numer. Methods Eng. **52**, 287–342, 2001)
39. Raviart, P.A., Thomas, J.M.: A mixed finite element method for 2nd order elliptic problems. In: Dold, A., Eckmann, B. (eds.) Mathematical Aspects of Finite Element Methods, Lecture Notes in Mathematics vol. 606. Springer, Heidelberg (1977)

40. Nédélec, J.-C.: Mixed finite elements in $I\!R^3$. Numer. Math. **35**(3), 315–341 (1980)
41. Nédélec, J.-C.: A new family of mixed finite elements in $I\!R^3$. Numer. Math. **50**(1), 57–81 (1986)
42. Monk, P.: Finite element methods for Maxwell's equations. In: Numerical Mathematics and Scientific Computation. Oxford University Press, Oxford (2003)
43. Bergot, M., Lacoste, P.: Generation of higher-order polynomial bases of Nédélec H(curl) finite elements for Maxwell's equations. J. Comput. Appl. Math. **234**(6), 1937–1944 (2010)
44. Savage, J.S., Peterson, A.F.: Higher-order vector finite element for tetrahedral cells. IEEE Trans. Microw. Theory Tech. **44**(6) (1996)
45. Mur, G., de Hoop, A.T.: A finite-element method for computing three-dimensional electromagnetic fields in inhomogeneous media. IEEE Trans. Magn. **21**(6), 2188–2191 (1985)
46. Elmkies, A.: Sur les éléments finis d'arête pour la résolution des équations de Maxwell en milieu anisotrope et pour des maillages quelconques, thèse de doctorat, U. de Paris Sud-Orsay (Paris XI) (1998)
47. Cohen, G., Monk, P.: Gauss point mass lumping schemes for Maxwell's equations. Numer. Methods Part. Differ. Eq. **14**(1), 63–88 (1998)
48. Yee, K.: Numerical solutions of initial boundary value problems involving Maxwell's equations in isotropic media. IEEE Trans. Antennas Propag. **14**(3), 302–307 (1966)
49. Cohen, G., Monk, P.: Mur-Nédélec finite element schemes for Maxwell's equations. Comput. Methods Appl. Mech. Eng. **169**(3–4), 197–217 (1999)
50. Cohen, G., Duruflé, M.: Non spurious spectral-like element methods for Maxwell's equations. J. Comput. Math. **25**(3), 282–304 (2007)
51. Demkowicz, L., Kurtz, J., Pardo, D., Paszynski, M., Rachowicz, W., Zdunek, A.: Computing with HP Finite Elements. II. Frontiers, Three-Dimensional Elliptic and Maxwell Problems with Applications. Chapman and Hall/CRC, London (2007)
52. Bergot, M., Duruflé, M.: High-order optimal edge elements for pyramids, prisms and hexahedra. J. Comput. Phys. **232**(1), 189–213 (2013)
53. Bergot, M., Duruflé, M.: Approximation of H(div) with high-order optimal finite elements for pyramids, prisms and hexahedra. Commun. Comput. Phys. **14**(5), 1372–1414 (2013)

http://www.springer.com/978-94-017-7759-9

Finite Element and Discontinuous Galerkin Methods for Transient Wave Equations

Cohen, G.; Pernet, S.

2017, XVII, 381 p. 79 illus., 39 illus. in color., Hardcover
ISBN: 978-94-017-7759-9